2015

Mechanical Behavior of Grouted Sands

Ryan C. Ortiz
University of Kentucky, ryan.ortiz@uky.edu

STUDENT AGREEMENT:

I represent that my thesis or dissertation and abstract are my original work. Proper attribution has been given to all outside sources. I understand that I am solely responsible for obtaining any needed copyright permissions. I have obtained needed written permission statement(s) from the owner(s) of each third-party copyrighted matter to be included in my work, allowing electronic distribution (if such use is not permitted by the fair use doctrine) which will be submitted to UKnowledge as Additional File.

I hereby grant to The University of Kentucky and its agents the irrevocable, non-exclusive, and royalty-free license to archive and make accessible my work in whole or in part in all forms of media, now or hereafter known. I agree that the document mentioned above may be made available immediately for worldwide access unless an embargo applies.

I retain all other ownership rights to the copyright of my work. I also retain the right to use in future works (such as articles or books) all or part of my work. I understand that I am free to register the copyright to my work.

REVIEW, APPROVAL AND ACCEPTANCE

The document mentioned above has been reviewed and accepted by the student's advisor, on behalf of the advisory committee, and by the Director of Graduate Studies (DGS), on behalf of the program; we verify that this is the final, approved version of the student's thesis including all changes required by the advisory committee. The undersigned agree to abide by the statements above.

Ryan C. Ortiz, Student

Dr. L. Sebastian Bryson, Major Professor

Dr. Y. T. Wang, Director of Graduate Studies

MECHANICAL BEHAVIOR OF GROUTED SANDS

THESIS

A thesis submitted in partial fulfillment of the
Requirements for the degree of Master of Science in Civil Engineering
in the College of Engineering
at the University of Kentucky

By

Ryan Christopher Ortiz

Lexington, KY

Director: Dr. L. Sebastian Bryson, Associate Professor of Civil Engineering

Lexington, KY

2015

ABSTRACT OF THESIS

MECHANICAL BEHAVIOR OF GROUTED SANDS

Grouting techniques have been in used for many years, but several new grout materials have surfaced in recent decades that have re-defined the boundaries of the limitations of grouting programs. Typically these applications are used for seepage control in earthen impoundments, but strength of these earthen impoundments should be considered where there is potential for movement in the grouted soil mass. This study investigated initial conditions that could affect grout application effectiveness. The initial conditions in question were soil grain size and in situ moisture content. Two grouts were used, ultrafine and acrylate, and variations in pure grout properties were studied. An apparatus was developed so that a uniform grout could penetrate the pore spaces of a soil specimen. The rate of penetration of the grout into the soil was studied. The unconfined compressive strength of the resulting grouted soil was then analyzed.

In testing neat ultrafine grout, it was shown that increased water-to-cement ratios had negative effects on the stability of the grout. Increasing the water-to-cement ratio from 0.5 to 2.5 resulted in a decrease in strength by a factor of 100. An inhibitor chemical was used to increase the time for reaction in the acrylate grout. During the chemical reaction, the curing temperature and gel times were monitored. A grout mix was selected for the acrylate grout that achieved appropriate gel times. In general, this study found that the grout penetrations rates into the soil increased as the initial moisture was increased from dry conditions to a gravimetric moisture content of nine percent. In each study, increased initial moisture decreased the grouted soil strength, with decreases in strength exceeding 50 percent. Empirical relationships were realized when compared to the initial matric suction of the soil. This suggests initial matric suction may be a useful initial condition for estimating increases in soil strength upon implementation of a grouting program for both the acrylate and ultrafine grouts.

KEYWORDS: Grouted sands, Acrylate, Ultrafine Cement, Grout Penetration, Strength.

Ryan C. Ortiz

March 23, 2015

MECHANICAL BEHAVIOR OF GROUTED SANDS

By

Ryan Christopher Ortiz

Dr. L. Sebastian Bryson
Director of Thesis

Dr. Y.T. Wang
Director of Graduate Studies

March 23, 2015

ACKNOWLEDGEMENTS

I would first like to acknowledge my advisor Dr. L. Sebastian Bryson. Dr. Bryson was not simply my research advisor, but the teacher and mentor who guided me in making crucial engineering career choices. He is the most inspiring teacher, and is responsible for sparking an interest in learning that I would never have achieved without his guidance. The time Dr. Bryson spent each and every day helping me realize and achieve my goals will always be cherished, as it is rare to find such a distinguished professional who is so devoted to ensuring that students succeed. His demonstration of how to be a top class professional while have fun and learning is an inspiration that I will carry with me the rest my life. I cannot express the depth of my appreciation for my four years spent researching on Dr. Bryson's research team and will be forever grateful.

I would also like to thank my professors at the University of Kentucky, who allowed me to expand my knowledge and ability to learn in the classroom: Dr. Michael Kalinski, Dr. Ed Woolery, Dr. Michael Kalinski, Dr. Y.T Wang, and Dr. Kyle Perry along with other professors at UK who guided me through my undergraduate career as well. I would also like to thank both Dr. L. Sebastian Bryson and Dr. Michael Kalinski for encouraging me to pursue the geotechnical engineering field through my interest in their courses and research experiences. I want to thank Dr. Kamyar Mahboub for my nomination for the Lyman T. Johnson Scholar. Professor Samantha Wright has been great mentor for my teaching assistantship and helped develop my graphical and spoken communication skills. The positions she entrusted to me were monumental in reaching my speaking and leadership aptitude, which will prove helpful ability as I transition into the workforce. Shelia Williams was instrumental in providing general support and doing

background work that made my research goals possible, and for that I am extremely thankful. The Civil Engineering Department at the University of Kentucky could not have been better for providing classes that kept me interested in engineering and providing every resource possible for the guidance of my education. I am very grateful for the education I have received at UK, and I appreciate the efforts by my professors in helping me earn my education.

My completion of my Master's degree would have not been possible without the help of my colleagues at the University of Kentucky. I would like to thank Xu Zhang, Corrie Walton-Macaulay, Ali Salehian, Isabel Gomez, Kirk Jenkins, Nishel'le Spencer, Jaquez Leandre, Malinda Jean-Louis, Jordan Keeney, Raghava Aditya, Alfred Susilo, Paul Smith and Kobina Sekyi for not only helping me with school related work but being friends as well. I would especially like to thank the team Bryson doctoral students, Corrie Walton-Macaulay, Ali Salehian, and Isabel Gomez, for providing support as student-mentors and showing me how to properly use the lab instrumentation.

Most importantly, I want to thank my family and close friends for their support in this journey. My parents, Ronald and Lisa Ortiz, provided constant support, without which none of my aspirations would be accomplished. My parents could not have been more supportive throughout my life, and luckily, new much better than I did about my potential life choice. Their guidance in these choices has proven and will continue to help me as I make my way. I want to thank my sister, Kaylee Ortiz, and uncle, Mike Ortiz, for their constant laughter and support. I especially thank my friends, who are too numerous to name, whose constant laugher and good times will continue throughout life. These people have made my life experiences full of joy and I am truly grateful. My

grandparents, Florencio Ortiz, Ileta Ortiz, Jim Reesor, and Noreida Reesor, truly instilled within me the desire to work hard, give back, love other people, and live life the right way. Without these people none of my accomplishments would be possible.

I would like to thank the Avanti International for supplying the materials used in the experimentation. I would like to thank U.S. Grout for manufacturing such chemicals and allowing me to experiment with ultrafine cementitious grouts. I. B. Moore donated the O-rings used in the experimentation, for which I am appreciative. I want to thank Nugent Sand Company for donating some of the sand used in this study.

Lastly, but foremost, I would like to thank God for without him nothing is possible. He has allowed us to decode minute portions of creation, in the form of physical sciences, and for allowing me to continue exploring at a graduate level.

TABLE OF CONTENTS

Table of Contents

LIST OF TABLES

LIST OF FIGURES

CHAPTER 1

1 Introduction

1.1 Background

Grouting has been utilized for the stabilization of earthen impoundments and foundations where seepage conditions are problematic or weak soil may fail. For geotechnical purposes, grouting programs have been used to stabilize weak soils, to contain hazardous waste, to erect low permeability grout curtains, to seal seepage in mines, re-stabilize tunnels, and to restore failing dams. In these stabilization applications, ordinary Portland cement grouts are often appropriate and are typically the first option considered (Babcock, 2013A). Ordinary Portland cement grouts have proven satisfactory in geotechnical solutions, such as seepage cutoff applications, where the effective grain sizes are greater than 1 millimeter (NAVFAC, 1983). In these applications, Portland cement has decreased seepage and stabilized weak soils. However, due to large cement particle sizes, ordinary Portland cement is ineffective for permeation grouting of medium and fine-grained sands, along with soils with significant fines (Zebovitz el al., 1989). Due to this ineffectiveness, several grouts have been developed that are capable of penetrating soils with finer particle sizes.

To grout soils with finer grain size distributions, chemical grouts were developed. This was because Portland cements are not applicable to conditions where fine sands exist. Chemical grouts can have viscosities similar to that of water, which allows permeation into some fine sands. Chemical grouted soils may exhibit satisfactory strength and excellent seepage control, but several issues exist with chemical grouts, such as the costs of such products are high and the longevity has been found to be less than that of cement. Due to these issues with chemical grouts, cementitious grouts with smaller particle sizes were developed to satisfy conditions where Portland cement may not be applicable. While cement grouts are cheaper, they sometimes fail to lower permeability. In these instances, chemical grouts may be applied after a cement grouting program, as critical locations where seepage reduction has not taken place (Babcock, 2013B)

Various forms of such grouts have been in use in recent decades. Grouting programs have shown to be effective in a variety of applications ranging from dam stabilization to

sealing mines (Soule and Henn, 2010). Also, several researchers have investigated the applicability of a variety of grouting material used for ground improvement applications (Karol, 2003; Warner, 2004; Powers et al., 2007). As grouts continue to be used for stabilization and ground improvement, the properties of the different grouts that exist should continue to be investigated, the factors affecting the mechanical behavior of the grouted mass must be investigated. For grouting applications that involve earthen impoundments, initial conditions of the soil, such as in situ moisture and density conditions, should be examined. With the anticipated increase in usage of this product, investigation into the effects that initial soil conditions may have on the strength of a grouted mass in earthen impoundments can benefit industry and the public good by contributing to sustainable design for infrastructure.

1.2 Basis of Study

1.2.1 Ultrafine Grout

Several useful studies involving cementitious grout materials have been published. Researchers Zebovitz et al. (1989) determined the groutability of sands based on variations of soil parameters, such as D_{15}, and formulated soil-specific relationships for ultrafine grouted sand permeability and unconfined compressive strength. However, the study did not study injection penetration rates into soil or the effects of initial soil conditions, such as in situ moisture and unit weight, in regard to grouted sand permeability and strength. Researchers Schwarz and Chirumalla (2007) studied the extent that constant, oscillating, and magnitudes of injection pressures affect the hydraulic properties and the strength of ultrafine grouted sand samples. However, these researchers did not evaluate any soil-specific initial conditions. Researchers Mollamahmutoglu and Yilmaz (2011) compared predicted groutability criterion versus experimental results, but did not present results of any experimentation of the resulting ultrafine grouted sand. The study found that poorly-graded grain size distributions, with few fines, are typically groutable. While a major benefit of ultrafine grout was its penetration ability into the soils with low hydraulic conductivity, the strength of the grouted soil mass was not thoroughly discussed.

While the primary consideration in design is that the earthen impoundment has adequate seepage reduction, quantification of expected strength is also important in design. Several researchers have investigated variation of strength parameters based on the grouting processes and initial soil conditions. Researchers Dano at al. (2004) established relationships in regard to unconfined compressive strength for various water-to-cement ratios, for ultrafine cement, as a function of relative densities of sand at one water-to-cement ratio. These researchers found a soil-specific cohesion and phi angle for two grouted sands. The only initial condition studied was relative density. Researchers Markou and Droudakis (2013) investigated unconfined compression data and grouted sand permeability when alterations were made in the water-to-cement ratio of the ultrafine grout and grain size of soil, having effective grain sizes ranging from 0.34 to 2.2. In regard to initial conditions, this study did not investigate initial soil unit weight and in situ moisture.

1.2.2 Acrylate Grout

Han et al. (2004) performed an experimental study on the gel time of acrylate grout and observed the chemical properties of the grout. A study performed by Krizek et al. (1980) tested various engineering properties of acrylate grouted sand, but did not look at variation in initial conditions of those properties. Additional research concerning acrylate grout should be performed, as this product is commercially available and used in various grouting applications (Avanti International, 2014A).

1.2.3 Unsaturated Initial Conditions

It is noted that the aforementioned studies typically assumed saturated conditions. While these mechanical studies have investigated many important groutability, grouted sand permeability, and strength relationships that exist for grouted sand, these studies have also highlighted the need for further research. The most evident need for further research are the effects of soil suction due and initial moisture conditions on grout penetration and strength.

Researchers Perret et al. (2000) investigated the effects of the degree of saturation on the ultrafine grout injection rate into sand along with the hydraulic conductivity of the grouted sand. These researchers also investigated suction and the soil matrix, along with

the resulting behavior of a grouted sand mass due to capillary effects. These researchers articulated and visually demonstrated the influence that the soil particle structure and water within the structure has on the grout penetration.

The aforementioned study demonstrated a need for further understanding of grout penetration into unsaturated media, the resulting strength, and quantification of strength due to variation of initial moisture conditions. This need is due to effects of dilution of the grout and effects of in situ suction on the resulting grouted sand. A major purpose of this study was to expand such knowledge.

1.3 Objectives of Research

The objectives of the grout research are as follows:

1) Quantify the effect that the grout mix design has on the pure ultrafine grout product

- ❖ This experimentation will verify what mix design is desired for the testing program. The results may provide insight into what mix designs are undesirable for select applications.
- Determine the extent that ultrafine cement grout mix design affects the water bleed of the grout
- Develop relationships for variation in cement grout mix design and strength
- Investigate the behavior that occurs in the chemical reactions that forms acrylate cured grout.
- Compare variations in grout chemicals and the resulting gel time and curing temperature
- Observe changes in gel time and curing temperature with variation in ambient temperature

2) Develop an apparatus that can be used to grout cylindrical soil specimens

- ❖ The important consideration of this portion is that the procurement of samples simulates that of field processes. This was executed by extensive review of previous research and applicable standards.
- Use previous studies and appropriate standards to create a apparatus to transport the grout through a porous medium

- Develop procedures so that the grout is distributed evenly within the pore spaces of the soil

3) Investigate the effect of initial conditions of soils and their effect on initial grout penetration
   - ❖ Understanding grout penetration into soil will contribute to the degree of effectiveness of grouting programs. This is because the success of the program is directly dependent the grout penetrates the soil adequately, filling the volume of soil desired by the project designer.
   - Determine the effects that grain size directly has on penetration into the pore spaces and groutability
   - Investigate the effects of initial moisture on the grout penetration into the soil specimen
   - Develop relationships in regard to penetration in regard to unsaturated soil mechanics
4) Develop relationships between soil initial conditions and the resulting grouted sand strength
   - ❖ The initial conditions of the soil could affect the strength of the grouted-mass. The degree of these effects should be quantified, to ensure grouting operations improve the soil to the necessary extent.
   - Explore the effects that different soil parameters have on strength of the grouted soil
   - Determine the extent that initial soil moisture changes grouted soil strength
   - Use unsaturated soil mechanics as a tool to estimate the effects of initial soil conditions on the grouted sand mechanical properties

1.4 Contents of Thesis

Chapter 2 presents a study concerning ultrafine grouts. Several properties of the grout were quantified. In particular for the neat ultrafine grout, the effect of water-to-cement ratio on engineering properties was investigated. Also, groutability data was presented and compared the existing groutability criteria. Grout penetration was investigated in regard to initial conditions. Properties of the in situ soil were related to the resulting grouted sand properties.

Chapter 3 presents an investigation regarding an acrylate-based grout. This study studied the pure grout, as it related to the curing of the grout. Specifically, a chemical was studied that prolongs, or inhibits, the time for the grout to gel was studied. Quantities of this inhibiting chemical were varied in the acrylate grout mix, and the gel time effects of this variation were quantified. This study also investigated the effects of the initial conditions on the acrylate grouted- sand. The effects studied were the grout penetration and ultrafine compressive strength of the post-grouted conditions.

Chapter 4 contains conclusions of this research.

Appendix A presents additional data for the soil indices obtained for the soils used in this study. This encompasses grain size distribution tables, specific gravity data, and hydraulic conductivity data.

Appendix B shows data that pertains to pure grout testing. For the neat cement, this pertains to bleed testing and unconfined strength testing. For the acrylate grout, the curing temperature and gel time were observed.

Appendix C shows pictures and processes use to grout the soil specimens, and associated grout penetration data. Pictures of the apparatus and associated procedures are outlined, and pertinent pictures are presented. Additional data regarding the grout mix penetrating the soil specimen is also shown.

Appendix D shows additional strength tables for the grouted sands.

Appendix E contains important information regarding product information for the grouting apparatus.

CHAPTER 2

2 Mechanical Behavior of Ultrafine Cement-Grouted Sands

2.1 Introduction

2.1.1 Grouting Introduction

Cementitous grout is used in the stabilization of foundations where weak soils exhibit behavior indicative of failure. Ordinary Portland cement grouts can be the appropriate solution for soil stabilization (Babcock, 2013A). In specialized geotechnical applications, such as in seepage cutoff, Portland cement grout has been shown to be effective for penetrating soils with effective grain sizes greater than 1 millimeter (NAVFAC, 1983). Due to grain sized limitations associated with Portland cement grout, previously described, requires the development of grouts with enhanced rheological properties.

Ordinary Portland cement has proven ineffective for permeation grouting of medium and fine-grained sands, along with soils with significant fines. This is due to large cement particle sizes associated with ordinary Portland cement, in relation to the pore spaces in medium and fine-grained sands (Zebovitz el al., 1989). In order to grout soils with finer grain size distributions, chemical grouts were developed. Chemical grouts have similar viscosities as water, which allows permeation into some fine sands. Chemical grouted soils may exhibit satisfactory strength and excellent seepage control, but the costs of such products are high and the longevity has been found to be less than that of cement. Also, some of these chemical grouts were banned in the past due to toxicity (Dano et al., 2004). Safety procedures in relation to toxicity have since been improved, but grout toxicity itself remains a sensitive design factor in the selection of a grouting program. Due to problems associated with cost and toxicity of chemical grouts, various cementitious grouts were developed that behave similarly to chemical grouts. One such cementitious grout is ultrafine cement grout.

2.1.2 Ultrafine Cement Grout Background

Ultrafine cement grout was developed to expand the limitations of grain and crack sizes that may be penetrated, while avoiding the cost, toxicity, and longevity issues associated with chemical grouts (U.S. Grout, 1999). Babcock (2013B) defines ultrafine cements as having a particle sizes ranging from three to five microns, while the particle size for

microfine cements have a particle size of six to ten microns (Backcock, 2013B). Ultrafine grout has enhanced rheological properties, better bleed properties, and sets in less time than ordinary Portland cement grouts (Henn, 2010). While academic studies and some in industry have distinguished between ultrafine and microfine grout, no industry or government standard has been formally developed (Babcock, 2014B). Due to the known effects of cement particle size on strength, a distinction has been made in this thesis between the terms microfine and ultrafine. In this study, ultrafine grout was selected, rather than a microfine grout.

For geotechnical purposes, ultrafine grout has been used to stabilize weak soils, to contain hazardous waste, to erect low permeability grout curtains, to eliminate seepage in mines, to control seepage in tunnels, and mitigate failing dams by forming seepage barriers. Several specific examples have shown benefit and applicability of ultrafine grout. In San Francisco, California, a team of engineers designed a permeation grouting operation to fortify the foundation of a historical church using ultrafine cement (Geo-Grout, 2008). In this application, the in situ soil was loose sand. Without geotechnical engineering intervention, the church's foundation would fail under seismic loading common in the area. The ultrafine grout was used to upgrade the foundations ability to withstand seismic forces. At a hazardous waste facility in Niagara Falls, New York, hydrologic evaluation showed that in order to protect public drinking water from toxic pollution, the existing natural waterways would need to be diverted from the facility to avoid contamination (Gazaway, 1991). A 26-meter deep by 820-meter long grout curtain was constructed, using ultrafine cement, in the path of the polluted waterway. The grout curtain successfully stopped the contaminant migration into the waterways. Grout curtains have commonly been used to reduce seepage and induce mechanical stability in dams. Ultrafine grout curtains were implemented at Rocky Reach Dam in Washington, United States, at a dam with silty sand foundation in Taiwan, and a dam protecting a mining operation in Argentina (American, 1960; Soule and Henn, 2010; Gentry and Magill, 2012). Furthermore, ultrafine grout has been shown to be effective in sealing tunnels and mines that have been compromised by significant amount of seepage, often in excess of 3000 liters per minute (Soule and Henn, 2010). It has been noted that the most common purpose of ultrafine grouting application is to reduce seepage. However,

mechanical behavior may continue to be studied, due to potential settlement and lateral movement of earthen impoundments. With the anticipated increase in usage of ultrafine cement, investigation into the effects that initial soil conditions have on the strength of a grouted mass in earthen impoundments can benefit industry and the public good by contributing to sustainable design for infrastructure.

2.2 Literature Review

2.2.1 Ultrafine Cement Grouted Soils

Previous studies have investigated grouting cylindrical soil specimens to quantify geotechnical characteristics of ultrafine cement grout, based on variation in grouting procedures and in situ conditions. The major convenience of ultrafine grout, as previously noted, was its lack of toxicity, cost, and ability to permeate (groutability) finer soils. Several studies analyzed the groutability and quantified the types of soils that can be grouted based on grain size.

Several useful studies involving groutability have been published. Researchers Zebovitz et al. (1989) determined the groutability of sands based on variations of soil parameters, such as the particle size corresponding to fifteen percent passing, and formulated a soil-specific relationship for grouted sand permeability and unconfined compression data of a grouted sand. However, these researchers did not study grout injection rates into soil and effects of initial conditions of the in situ soil, such as unit weight or moisture content. Researchers Schwarz and Chirumalla (2007) used variable injection pressures. In particular, these researchers used constant and oscillation injection pressures, and also varied the magnitude of the injection pressure. These researchers investigated the grout penetration properties along with the strength of grouted sand samples, in comparison to variable injection pressure types and magnitudes. However, these researchers did not look at any soil-specific initial conditions. Researchers Mollamahmutoglu and Yilmaz (2011) examined predicted groutability criterion versus experimental results, but did not inspect the resulting grouted sand. These researchers concluded that poorly-graded grain size distributions, with few fines, are typically groutable. While a major benefit of this grout, in improvement of weak soils, is its penetration ability into the soil and low

hydraulic conductivity, the strength of the grouted soil will continue to be an important design consideration.

While the primary consideration in design is that the underground structure has adequate seepage reduction, quantification of expected strength will be important in design. This is because settlement and lateral movement are possible in earthen impoundments, such as dams. Several researchers have investigated variation of strength parameters based on the grouting processes and initial soil conditions. Most studies tested specimens at saturated conditions. Researchers Dano at al. (2004) established relationships in regard to unconfined compression for water-to-cement ratio, relative density at one water-to-cement ratio, and have found a soil-specific cohesion and phi angle for two grouted sands. However, the only initial condition studied was relative density. Researchers Markou and Droudakis (2013) investigated unconfined compression and grouted sand permeability when alterations were made in the water-to-cement ratio of the grout and grain size of soil; for initial conditions, this study investigated a range of grain sizes. This study investigated soils with D_{15} values ranging from 0.13 to 0.43 mm, but did not present any relationships in pertaining to grain size. The range of grain sizes explored can be expanded. These mechanical studies have extensively verified many important groutability, grouted sand permeability, and strength relationships that exist for grouted sand; these have also sparked the need for further research.

2.2.2 Importance of Specific Research

As has been presented, several studies attempted to quantify some of the relationships between engineering properties and grout injection, soil types, and conditions. Still, there are some conditions yet to be investigated. Most notably are the effects of soil suction due to initial moisture conditions on grout penetration and strength. Researchers Perret et al. (2000) investigated the effects of the degree of saturation on the injection rate into sand along with the grouted sand permeability; these researchers investigated suction and the soil matrix, along with the resulting behavior of a grouted sand mass due to capillary effects. These researchers articulated and visually demonstrated the influence of the soil particle structure and the water content within the structure has on the grout penetration. However, no specific relationships were developed and insufficient testing was

performed in order to develop such relationships. While the study did look at initial moisture characteristics, it did not directly measure suction. The aforementioned study demonstrates a severe need for further understanding of grout permeation into unsaturated media, the resulting strength, and quantification of strength due to variation of initial moisture conditions.

2.3 Testing Materials

2.3.1 Test Sands

2.3.1.1 Index Properties

A test program was developed to provide a basic understanding of the role of unsaturated soil mechanics on engineering properties of grouted sands. To achieve this objective, five different sands with varying grain size characteristics were tested. The grout injection into the sands was monitored and the grouted sand strength was tested after the specimen cured. The grain size distribution curves for the sands selected for use in this study are shown in Figure 2.1. As discussed earlier, previous studies developed relationships for various grain size parameters.

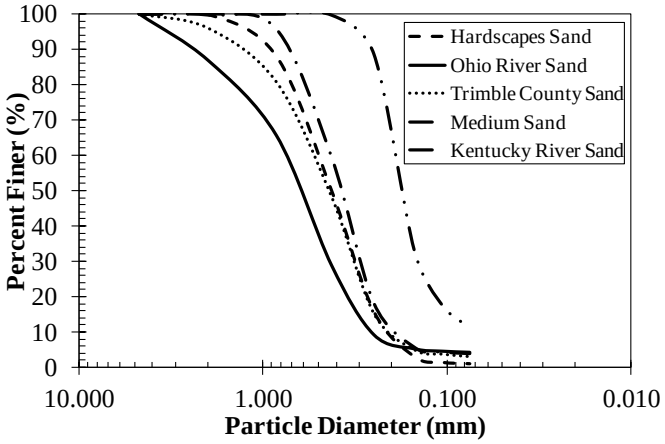

Figure 2.1. Grain Size Distribution.

In previous research conducted by Markou and Droudakis (2013), effective grain size (D_{10}) values ranging from about 0.34 to 2.15 millimeters were analyzed. To compliment previous research, soils with finer grain sizes were selected for investigation in this study. The range of D_{10} values in this study range from 0.18 to 0.28 millimeters. The specific gravity values, presented in Table 2.1, are typical values for sands. Kentucky River sand is naturally occurring sand. This sand is classified as fine grained and has a substantial

amount of fines, which may be responsible for its high specific gravity. Ohio River sand is also naturally occurring sand. However, this is coarse sand. Hardscapes sand is mechanically altered manufactured sand and is commercially available. This sand has a medium grain size. Medium sand is naturally occurring and was mechanically altered. Trimble county sand is naturally occurring. Relevant grain size data is presented in Table 2.1.

Table 2.1. Sand Data.

Sand Name	Specific Gravity, G_s	D_{60} (mm)	D_{30} (mm)	D_{10} (mm)	Coefficient of Curvature, C_c	Specific Surface Area, S_s (mm^{-1})
Kentucky River Sand	2.69	0.18	0.13	0.07	1.3	38.1
Ohio River Sand	2.66	0.73	0.42	0.36	0.7	15.1
Hardscapes Sand	2.65	0.48	0.31	0.22	0.9	19.1
Medium Sand	2.66	0.4	0.28	0.18	1.1	20.7
Trimble County Sand	2.66	0.5	0.32	0.22	0.9	17.8

Coefficient of curvature (C_c) and specific surface area (S_s) values have been presented in Table 2.1. The coefficient of curvature is used to provide an index of the gradation, or the distribution of particle sizes within the sample. Coefficient of curvature is defined as

$$C_c = \frac{D_{30}^{\ 2}}{(D_{10} \times D_{60})} \tag{1}$$

where D_{10} is the particle size corresponding to 10 percent passing, D_{30} refers to the particle size corresponding to 30 percent passing, and D_{60} is the grain size corresponding to 60 percent passing. Specific surface area is a index of the surface area of the particles in a soil specimen.

$$S_s = \frac{SF}{D_{eff}} \tag{2}$$

where SF is a shape factor, commonly 6 for round-grained soils, and D_{eff} is the effective diameter. The effective diameter is

$$D_{eff} = \frac{100\%}{\sum \frac{\Delta F_i}{\sqrt{D_{max,i} D_{min,i}}}} \quad (3)$$

where $D_{min,i}$ is the minimum grain size for a selected interval, $D_{max,i}$ is the maximum grain size in a selected interval, and ΔF_i is the percentage correspond to the selected grain size interval.

2.3.1.2 Hydraulic Properties

Saturated hydraulic conductivity testing was performed to understand the characteristics of the soil. All tests were performed in accordance to ASTM D4234. The saturated hydraulic conductivity values of the soils used in the study are shown in Table 2.2.

Table 2.2. Saturated Hydraulic Conductivity.

Sand Name	Saturated Hydraulic Conductivity, k_s (m/s)
Kentucky River Sand	2.5E-06
Ohio River Sand	4.4E-04
Hardscapes Sand	3.5E-04
Medium Sand	2.6E-04
Trimble County Sand	3.8E-04

The unit weight of the specimens was 15.7 kN/m^3, which was constant throughout this study. These hydraulic conductivities are similar to those found in other studies (Markou and Droudakis, 2013; Perret et al., 2004). Common tests for hydraulic conductivity are limited to saturated soils. A study by Hazen (1892) found that hydraulic conductivity was highly correlated to effective grain size squared, D_{10}^2. The results, in this study, between hydraulic conductivity versus a grain size factor squared, D_{10}^2, are shown in Figure 2.2. The Hazen (1892) equation is

$$k_s = CD_{10}^{\ 2} \quad (4)$$

where k_s is hydraulic conductivity and D_{10} is effective grain size, or the grain size that 10 percent of the particle size distribution is finer than. Emperical coefficient "C" is an empirical coefficient equal to 0.5. The empirical coefficient is unique to the data and specific to the range of effective grain sizes presented.

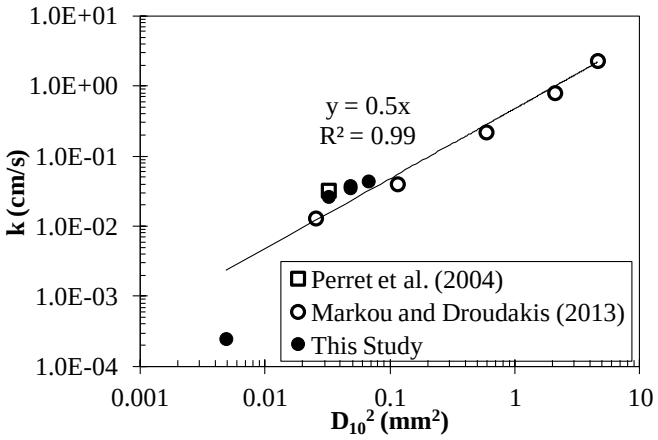

Figure 2.2. Hydraulic Conductivity versus Grain Size Factor, D_{10}.

Coefficient "C" represents the rate of increase per unit D_{10} increase, where hydraulic conductivity increase 0.5 cm/s per 1 mm effective grain size increase. The high correlation coefficient for this empirical equation of hydraulic conductivity with effective grain size shows why grain sizes are often attributed to groutability of soil. It should be noted that while a constant dry unit weight was used in this study, the dry unit weight corresponding to data in other studies may vary.

2.3.1.3 Soil-Water Characteristics Curves

Due to variability with in situ moisture content, unsaturated soil mechanics was a major interest for this study. Unsaturated soil mechanics quantifies the effects of soil moisture on matric suction, which provides insight into other engineering properties. Specific to this study, unsaturated soil mechanics provided insight into grout penetration rates during the grout injection phase of the experimentation and provided insight into the mechanical behavior of grouted sands.

The soil-water characteristics curve (SWCC) is the fundamental interpretive tool to analyze effects of water in the soil skeleton (Fredlund et al., 2012). SWCCs are soil-specific relationships between suction and moisture. These curves are non-unique solutions and have variability based upon initial unit weight, wetting versus drying, and the type of pore fluid. The Fredlund and Xing (1994) expression was used to interpret volumetric water content and suction data in order to develop a SWCC curve. The expression utilizes a parameter optimization procedure that gives non-unique solutions, which are highly dependent upon the input data and the optimization constraints. Two

equations are used in the optimization procedure. One equation is used to estimate the volumetric water content

$$\theta = C(\psi)\left[\frac{\theta_s}{\left\{\ln\left[e+\left(\frac{\psi}{a}\right)^n\right]\right\}^m}\right] \tag{5}$$

where θ is volumetric water content, θ_s is volumetric water content at saturation, and e is 2.718. Variables a, n, and m are fitting parameters obtained by the SWCC optimization method. Volumetric water content is

$$\theta = w\left(\frac{\gamma_d}{\gamma_w}\right) \tag{6}$$

where w is gravimetric moisture content, γ_d is the dry unit weight, and γ_w is the moist unit weight. The second equation, $C(\psi)$, is a correction function. This function is

$$C(\psi) = 1 - \frac{\ln\left(1+\frac{\psi}{\psi_r}\right)}{\ln\left(1+\frac{\psi_d}{\psi_r}\right)} \tag{7}$$

where ψ is matric suction, ψ_r is the residual matric suction, and ψ_d is dry matric suction. The dry suction, ψ_d, was a constant, and is 1,000,000 kPa. The resulting SWCCs, shown in Figure 2.3, were obtained using a Microsoft Excel Equation Solver and direct volumetric water content measurements using a Tempe cell. Parameters obtained from the analysis are presented in Table 2.3. The residual suction, ψr, was held constant at 100 kPa for coarse grain graded soils, as suggest by the Fredlund (1999) for initial conditions. Fitting parameters “a”, “n”, and “m” were bound between 1 to 15150, 1 to 20, and 0.5 to 4, as recommended by Fredlund and Xing (1994).

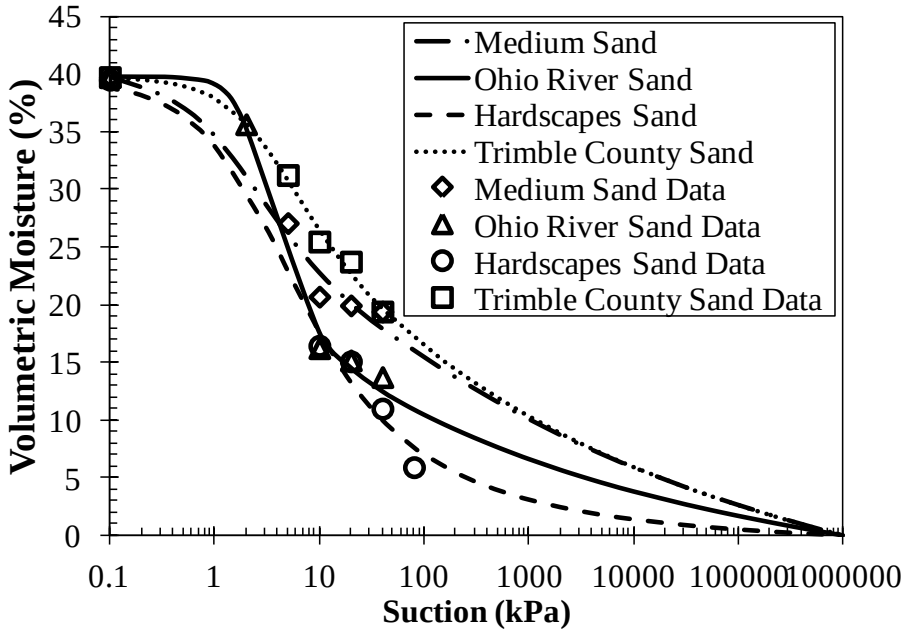

Figure 2.3. Fredlund and Xing (1994) Optimized Fit for Test Sand.

Several researchers have shown that the SWCC parameters correspond to grain size indeces. Torres (2011) showed that the Fredlund and Xing (1994) a-parameter correlated to D_{10}. The relationship in this study between "a" and D_{10} is shown in Figure 2.4.

Table 2.3. Soil Water Characteristics Curve Parameters.

Sand Name	Saturated Volumetric Water Content, θ (%)	Air Entry Value, ψ_{aev} (kPa)	Fitting Parameter, a	Fitting Parameter, n	Fitting Parameter, m
Medium Sand	39.8	0.7	1.0	1.2	0.5
Ohio River Sand	39.8	1.4	2.1	3.2	0.5
Trimble County Sand	39.8	1.4	2.6	1.4	0.5
Hardscapes Sand	39.5	13	2.6	1.0	1.3

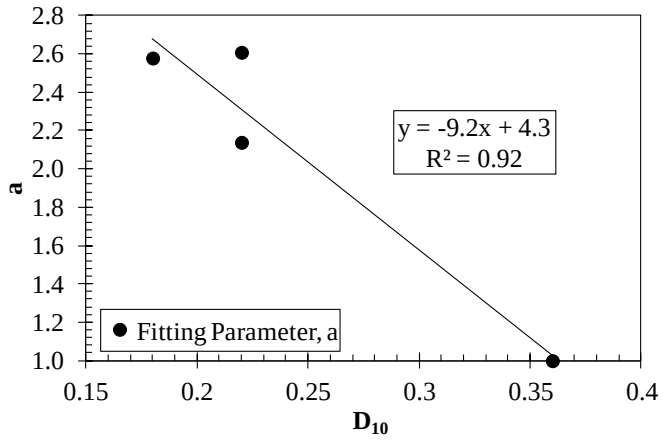

Figure 2.4. Fitting Paramter, a, versus D_{10}.

An empirical relationship relating fitting parameter "a" and D_{10} has been shown. This relationship exists because grain size significantly affects the SWCC curve. As presented, with the initial unit weight, of 15.7 kN/m^3, in each of the soils, the grain size has a significant effect on the curve. As such, the fitting parameter "a" decreases as effective particle size increases.

2.3.1.4 Hydraulic Conductivity of Unsaturated Soils

In unsaturated soil mechanics, unsaturated measures of hydraulic conductivity have proven useful in demonstrating flow behavior in partially saturated soils. Relative hydraulic conductivity is a parameter often used to estimate the degree of unsaturated conductivity variation relative to the saturated hydraulic conductivity. This parameter is defined as

$$k_r = \frac{k_w}{k_s} \tag{8}$$

where k_w is the unsaturated hydraulic conductivity and k_s is the saturated hydraulic conductivity. Figure 2.5 shows how the relative hydraulic conductivity varies with volumetric moisture. This is because volumetric moisture is related to suction. Suction was used to calculate the relative hydraulic conductivity. Figure 2.5 does not show one unique solution, but four individual trends, therefore, no empirical relationship has been included.

Relationships have been presented that estimate unsaturated hydraulic conductivity using parameters obtained from the SWCC curve and matric suction values that correspond to the in situ moisture conditions (Fredlund, 2006). One such hydraulic conductivity relationship, presented by Campbell (1974) was of particularly applicable to this study because it applies a closed form solution based on the air entry value to estimate relative hydraulic conductivity, k_r. The Campbell (1974) relationship is

$$k_r = (\psi_n)^{(-4/b)} \tag{9}$$

where k_r is relative hydraulic conductivity, b is a constant, and ψ_n is normalized suction. In Equation 9, $b = \ln(\psi_0)$. Suction at dry conditions, ψ_0, is 1,000,000 kPa. This equation provides reasonable results into the transition zone of the SWCC (Fredlund, 2006).

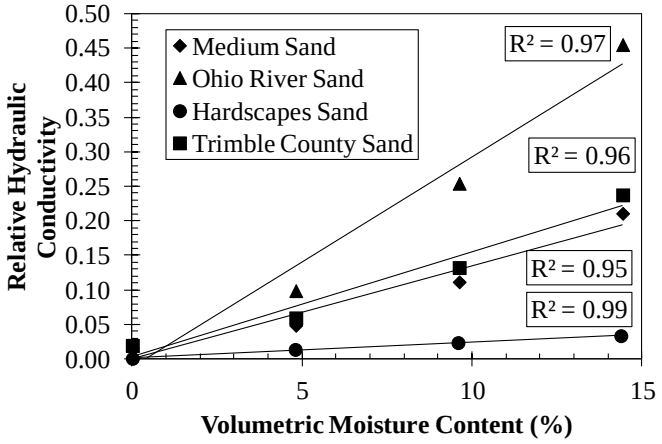

Figure 2.5. Relative Hydraulic Conductivity versus Volumetric Moisture Content.

Relative hydraulic conductivity was known to increase with volumetric moisture in the same manner shown in Figure 2.5. This relationship was due to the changes in matric suction with moisture. Shown in Equation 10, the moisture-specific suction value was normalized to the air entry value. Normalized suction is

$$\psi_n = \frac{\psi}{\psi_{aev}} \tag{10}$$

where ψ_{aev} is the air entry value and ψ is the suction at a corresponding volumetric water content selected from the SWCC.

2.3.2 Ultrafine Grout

2.3.2.1 Ultrafine Grout Properties

The ultrafine grout used in this study was Type V Standard Grout. The grout was manufactured by U.S. Grout, LLC and distributed by Avanti International. By weight, the ultrafine cement grout contained 55 percent pumice, 45 percent Portland cement, and 0.09 to 0.12 percent modified polymer powder. In the ultrafine cement, 90 percent of the particles sizes are distributed below 8 microns and the average particle size was 4 microns. The ultrafine cement mixing instructions include a 0.6 water-to-cement ratio by weight. For this water-to-cement ratio, the initial gel and workability ranges from 2.5 to 5 hours and the set time ranges from 4.5 to 7 hours. This ultrafine cement grout yielded optimum properties in regard to the penetration ability, cement setting times, groutability, and workability for the purpose of grouting sands.

2.3.2.2 Neat Grout Testing

In cement suspensions, water has a tendency to segregate from the mix. This tendency is termed bleed. Often, the bleed is referred to as stability, because the bleed has a direct effect on the stability of grout. Several factors that affect water segregation are the grout properties, such as the cement particle specific surface area and the water-to-cement ratio. Increasing the water-to-cement ratio will increase the amount of bleed from the suspension. Typically, in construction applications the highest water-to-cement ratio used is two, due to the increased bleed characteristics and decrease in strength properties (Henn, 2010). Ultrafine cements have a reduced tendency for water separation than other cement grouts. The fine grained particles in ultrafine cement react with the water fast and have lower potential for gravitational settlement. Thus, ultrafine grout mixtures with significantly higher water-to-cement ratios, than that of grouts with larger particle sizes (ie. ordinary Portland cement), have been used to grout underground formations and in academic studies (Zebovitz et al., 1989; Dano et al., 2004; Saada at al., 2006; Schwarz and Chirumalla, 2007; Kim and Whittle, 2009 Markou and Droudakis, 2013).

A neat grout testing program was implemented to observe bleed and test neat grout samples in unconfined compression. The samples were formed in split-molds, and allowed to set for 24 hours. The original testing program observed the bleed for four

samples, containing water-to-cement ratios of 1, 2, 3, and 4. For verification of the bleed characteristics, the testing program was repeated at the same water to cement ratios. As such, the bleed data corresponding to the water-to-cement ratios was repeated. This can be seen in Figure 2.6, where there are two data points corresponding to water-to-cement ratios of 1, 2, 3, and 4, yet the corresponding data points plot at nearly the same point. To further verify the results of this experiment, Henn (2010) data has also been included in the relationship. The Henn (2010) contained Nittetsu Superfine grouting mixed at a water –to-cement ratio of 3 and DeNeef MC=500 grout mixed at water to cement ratio of 4.

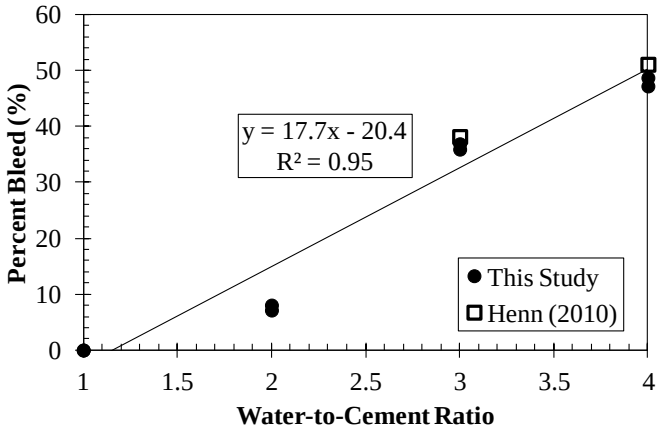

Figure 2.6. Effect of Water-to-Cement Ratio on Grout Bleed.

The equation relating percent bleed to variation in water-to-cement ratios is

$$\beta = c_1\left(\frac{W}{C}\right) + c_2 \tag{11}$$

where β is the percent bleed, W/C represent the water-to-cement ratio, $c_1 = 17.7$, and $c_2 = -20.4$. The constants c_1 and c_2 are empirical constant based on these experimental results. Empirical constant c_1 was the rate at which the water separates from the mix for different samples with variable water-to-cement ratio. As the water-to-cement ratio was decreased, a point was reached where no bleed takes place. This was where the line intercepts the x-axis. The water-to-cement ratio where no bleed takes place, estimated from Equation 11, is 1.2. As previously described, a water-to-cement ratio equal to two is commonly used in applications and in laboratory experiments (Henn, 2010). This is why this ratio is

commonly used in the field. Figure 2.6 shows data that correspond to a water-cement ratio of 2 was at approximated 7.5 percent bleed.

Unconfined compression tests were performed on the neat grout samples. The tests were performed in accordance to ASTM D4320, as were all unconfined tests performed in this study. Unconfined compressive strength as a function of water-to-cement ratio is shown in Figure 2.7. In the figure, water-to-cement ratios from 0.5 to 2.5 are shown.

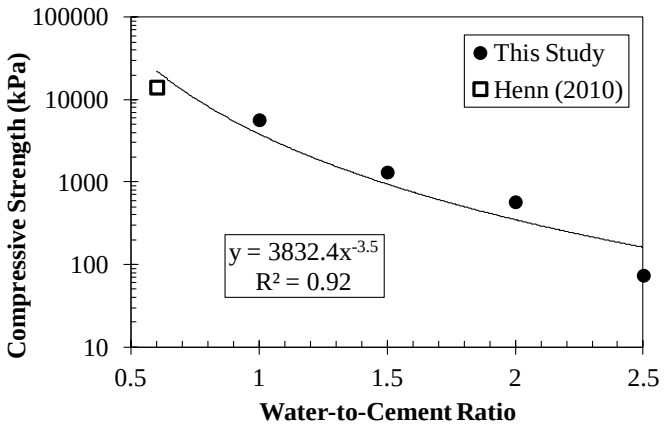

Figure 2.7. Relationship between Unconfined Compressive Strength versus Water-to-Cement Ratio.

Dano et al. (2004) proposed an equation that related the unconfined compressive strength of neat grout to water-to-cement ratio as a power function. The equation found in this study is also a power function. However, a different grout was used and the parameters found were different. This equation found in this study for the unconfined compressive strength with variation in water-to-cement ratio for the ultrafine cement grout used is

$$q_{u(ng)} = A_0\left(\frac{W}{C}\right)^{-N} \tag{12}$$

where $q_{u,(ng)}$ is the unconfined compressive strength of the neat grout, W/C is the water-to-cement ratio, and A_0 and N are empirical constants based on the experimental data. For the grout used in this study, A_0 = 3832.4 and N = 3.5. Henn (2010) data was included in the relationship, as the data was obtained using the same type of grout used in this study.

In Figure 2.7, a power function was used to describe the relationship for strength with variations in the water-to-cement ratio of the grout. The empirical constants describe the

behavior of the grout strength with this variation. Empirical constant A_0 simply represents the compressive strength when the water-to-cement ratio is one. This is because when you sub a water-to-cement ratio into Equation 12, you get the same value as parameter A_0. Empirical constant N represents the power function rate of decrease in strength as the water-to-cement ratio decreases.

2.4 Grouting Apparatus

A grouting procedure was developed so that a uniform grout could permeate cylindrical soil samples. In this procedure, the grout was allowed to set within the sample and to ensure the sample was undisturbed. The apparatus used in the procedure was constructed based on specifications in ASTM D4320. Any variances from this ASTM will be noted. A schematic of the apparatus is given in Figure 2.8.

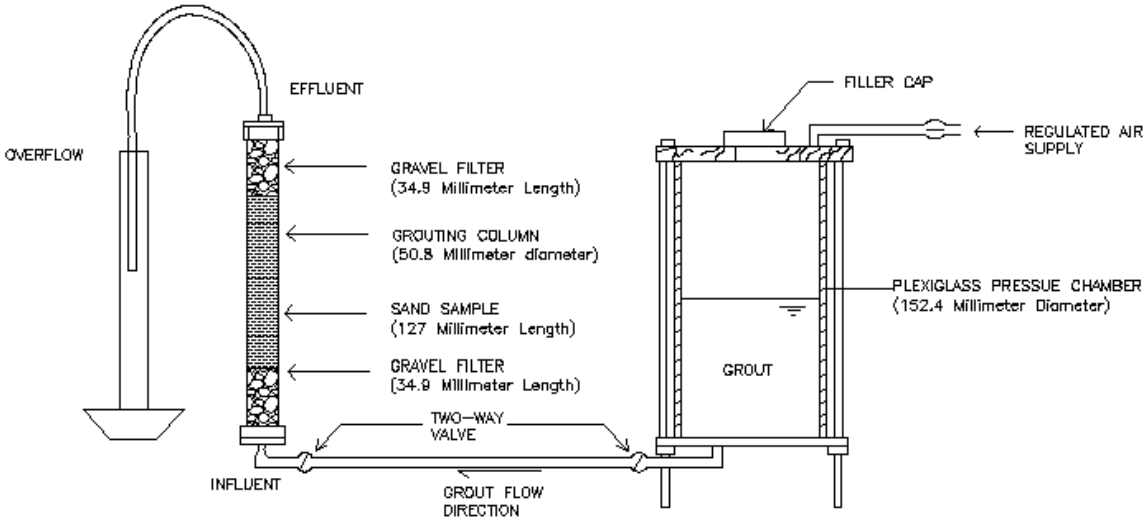

Figure 2.8. Schematic of Grouting Apparatus.

A DurhamGeo 152.4 millimeter constant/falling head permeameter was used as a pressure chamber. No stirring mechanism was utilized in the grout tank, as sample penetration occurred quickly upon pressurization. The grout tank was pressurized at the top and the grout flowed from the bottom to the influent of the sample. A two-way valve was attached to the bottom of the tank, so that the liquid ultrafine cement suspension could be held in the tank as pressure was initiated. This was important, because the regulated air pressure supply decreased as the influent air pressure was turned on. The regulated air pressure supply was allowed to increase to the appropriate pressure prior to

opening the two-way valve. Upon engagement of the two-way valve, the grout instantly permeated through the soil.

The apparatus utilized an appropriately sized acrylic tube and acrylic sheet as the grout column and bases for the column. The bases were threaded to accommodate appropriate fittings. The bases contained machined, circular grooves so that o-rings could be inserted into the bases. The bases were machine threaded, in order for the effluent and influent fittings to be attached. The cylindrical acrylic-mold had a 50.8 millimeter diameter and 201.6 millimeter length. However, the total sample length was 196.8 millimeters, because the molds fit 3.2 millimeters into the bases.

Wax paper was placed around the sample directly inside the cylindrical acrylic mold. The sand samples, as placed in the mold, had a length of 127 millimeters. Situated on the top and bottom of the samples was 34.9 millimeters of gravel, directly above the influent and below the effluent. This gravel layer was used as filter media so the sand sample did not clog the influent and so that sand did not travel with the grout through the effluent. A constant dry unit weight of 15.7 kN/m^3 was used for the sand samples throughout this study. For Ohio River sand, Trimble County sand, and Hardscapes sand, no compaction was required for dry samples. In the moist samples, ranging from three to nine percent gravimetric moisture, ten tamps were used per layer for three layers. In the medium sand, the dry sand was compacted in four layers with ten tamps each, tapping the sides of the mold ten times per layer. In the moist samples for the medium sand, the samples were compacted in eight layers with twenty tamp on each layer and twenty taps on the side of the mold for every other layer. Wire mesh was placed in between the gravel and influent, the gravel and sand sample, and in between the gravel and effluent.

As the grout exits the sample effluent, the ultrafine grout flows into a graduated cylinder for discharge measurements. Grouting was continued to 200 milliliters or until refusal. Refusal occurred when no flow was apparent from into the effluent graduated cylinder. The cylinder, filled with the uncured grouted sand, was transported and placed between two rubber mats to ensure no grout leaks occurred. The sample was allowed to set for 24 ± 6 hours then was placed in a humidity curing chamber. The samples were extracted by pushing the samples out using a hydraulic press. The wax paper surrounding the sample,

which was previously described, was used to eliminate side friction upon extraction. Cured grouted samples were capped using a sulfur compound to create a smooth contact surface between the compression platens. The samples were strength tested seven days from the date of mixing.

2.5 Hydraulic Characteristics

2.5.1 Groutability Criteria

For a sample to be groutable, the void space of the soil specimen must accept the grout suspension. Several factors that govern grout penetration behavior are widely accepted in the grouting community. The percentage of fines has been shown to cause the soil to refuse grout. It has been widely noted that soils with ten percent or more fines may be problematic when grouting attempts are made. Problems grouting soils with as low as five percent fines have also been noted in academic studies (Zebovitz et al, 1989). Another major factor in groutability is the cement-soil particle size ratio, or the ratio of the cements largest particles to the soil's smallest particles. Past studies have shown that grout penetration in soil is highly dependent on the smaller voids in a soil formation and the larger particles in the grout material (Johnson, 1958; Scott, 1963; Mitchell, 1970).

One of the more commonly accepted criterion, that takes particle sizes of the cement and soil into consideration, is the groutability ratio (Axelsson and Gustafson, 2007; Henn, 2010; Mollamahmutoglu and Yilmaz, 2011). The most common criterion has been suggested by Henn (2010). This equation is

$$N = \frac{(D_{15})_{soil}}{(D_{85})_{grout}} \tag{13}$$

where N is the groutability ratio, $(D_{15})_{soil}$ is the grain size corresponding to 15 percent finer by weight of the soil, and $(D_{85})_{grout}$ is the grain size corresponding to 85 percent finer by weight of the grout. For this criterion, if N is greater than 24, grouting should be possible. If N is between 11 and 24 grouting may be possible. If N is less than 11, grouting will not likely be possible. For the material used in this study, the manufacturer designates 8 microns as the cement grain size corresponding to 90 percent finer by weight. This grain size value will be used for $(D_{85})_{grout}$, since this will provide a

conservative estimate of groutability. Figure 2.9 shows the calculated N value for each soil, and what groutability designation it corresponds to.

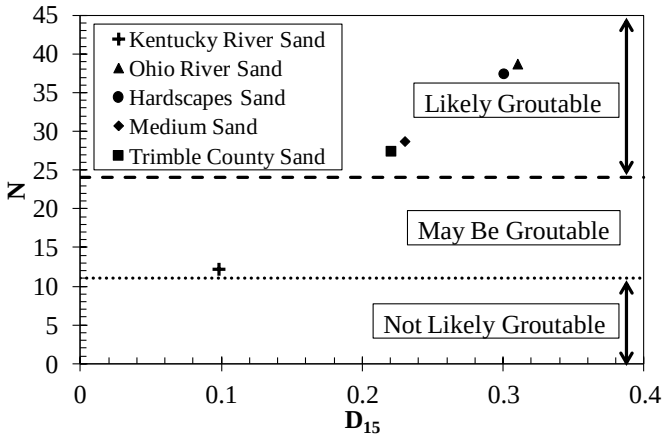

Figure 2.9. Groutability Factor versus Grain Size for 15 Percent Passing.

Kentucky River sand has a groutability ratio of 12.3. This groutability ratio indicates grouting may be possible. The groutability ratio for Kentucky River sand indicates this soil was much closer to classification "not likely groutable" than classification as "likely groutable". While no distinct criteria exists that relates ultrafine cement groutability and fines, various predictive measures for determination of groutability exist for chemical grout and fines. These measures have designated soils with less than ten percent sands groutable, and soils with ten to twenty percent fines moderately groutable (Powers, 2007; Henn, 2010). Using the fines criteria for groutability using chemical grouts, Kentucky River Sand was moderately groutable. The remaining sands are considered groutable, similar to the results for groutability ratio. These predictive measures are for chemical grout, but can be used to predict behavior for cement grouts with caution. Various criteria based on grain size exist that give indications of groutability, but none give a decisive indication of groutability.

2.5.2 Grout Injection

2.5.2.1 Test Setup

In order to assure that soils are mechanically improved to satisfy design recommendations in the field, laboratory tests are commonly carried out to predict the strength. A major consideration for laboratory testing was that grouting material must be uniform throughout the sample specimen in question, such as is assumed to be the case in

field applications. Typically this has been performed by pumping, or injecting, a grout through a soil sample. The apparatus and procedure previously described were used to meet these requirements. During injection of the grout into the soil specimen, measurements were used to quantify penetration effects in the test soils with the intent that they may be able to be related to field techniques through the progression of grout research.

2.5.2.2 Test Results

Grout injection theory has been reviewed in detail by various sources (Bell, 1993; Karol, 2003). Very little research has been performed to develop relationships based on this theory. In uniform, isotropic soils, grout has typically been injected from a perforated, pressurized column and permeates laterally (Littlejohn, 1985; Xanthakos et al., 1994). The initial injection rate, or penetration rate, was the major concern of this study, because in the field this will have a significant effect on penetration radius. In this study, the penetration rate was the time it took the grout to permeate through the length sample from influent to effluent. This time for this permeation is presented as length over time. If the factors effecting grout penetration in a porous medium can be determined, these same factors will affect lateral penetration in the field. In this study, the initial moisture content of the soil samples were varied prior to grouting. Perret et al. (2000) performed a case study looking at effects of moisture on grout permeation. The penetration in these soils increased with as moisture in the soil increased. The cause of the increased rates of penetration with increased moisture was attributed to mixing of grout with the in situ water and changes in the suction of the soil. Adsorption associated with dry soils causes penetration rates to be low, as has been seen in previous research (Abraham, 2006). These trends for grout penetration rates at various volumetric moisture contents are seen in Figure 2.10. It was noted that some of the soil specific trends intersected, just after dry conditions. This may be due to the adsorption characteristics of specific soil particles, where a more adsorbent soil exhibits lower penetration rates. As the moisture was increased, the soil specific suction controlled behavior.

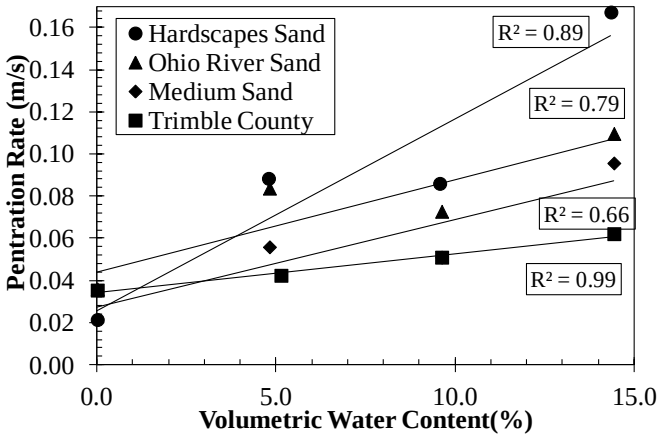

Figure 2.10. Normalized Penetration Rate versus Volumetric Water Content.

As previously described, soil suction varies as the in situ volumetric moisture content is changed. Figure 2.11 shows the relationship between penetration rate and suction in this study. This relationship yields empirical equations. In this empirical equation, penetration is

$$P_R = b_1(\psi)^{b_2} \tag{14}$$

where ψ is suction and b_1 and b_2 are empirical constants equal to 0.15 and -0.1. Parameter a_1 corresponds to a suction value of 1, as subbing in 1 for the suction value results in a P_R that is equivalent to b_1. Parameter b_1, physically, is the rate of change in penetration per unit suction. Suction is related to the penetration rate because suction takes in situ soil characteristics, such as unit weight, moisture content, and grain size, as previously discussed. While suction may be a useful tool in predicting grout penetration, additional influences from the grouting program, such as injection pressure and the grout viscosity, should also be considered when developing relationships in regard to grout penetration of soils.

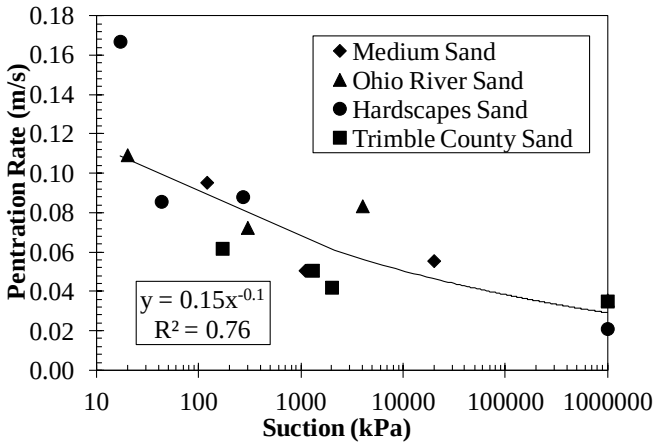

Figure 2.11. Penetration Rate versus Suction.

Flow through a porous media has been theorized using Darcian and Newtonian theory (Xanthakos et al., 1994). A Bingham flow criterion has been previously used by researchers to determine groutability and flow for bentonite suspensions and cementitous grouts that have low water-to-cement ratios, such as 0.6. However, Newtonian flow was valid for this research study, as a water-to-cement ratio of two was used for reasons previously stated. Early grout research realized and quantified the necessary hydraulic head to grout soils based on soil hydraulic conductivity, grout viscosity, injection source diameter, and desired grout penetration radius (Raffle and Greenwood, 1961). A relationship proposed by Maag (1938) was used in conjunction with the hydraulic head equation to add a porosity component to this relationship and simplifies the equation. This equation is

$$t = \frac{\mu n}{3kHr} V_g \tag{15}$$

where μ is grout viscosity, n is porosity, k is the hydraulic conductivity, H is the hydraulic head, r is the injection radius, and V_g is a volume term representing the volume to be grouted. In Equation 15, the grout volume is

$$V_g = R^3 - r^3 \tag{16}$$

where R is the grout penetration radius, whereas in this study, the grout volume is

$$V_g = LR^2\pi \tag{17}$$

For the samples in this study, the volume component of the equation was the volume of a cylinder. As indicated, components of Equation 15 were used to develop a factor used to quantify a relationship between grout penetration and initial conditions of the soil. The length and time terms were isolated on one side, and the viscosity and hydraulic conductivity were normalized. The resulting parameter is

$$K_F = \frac{k_r H r}{\left(\frac{\mu_g}{\mu_w}\right)\pi R^2 n} \tag{18}$$

where k_r is relative hydraulic conductivity, H is pressure head, r is the injection radius, μ_g is grout viscosity, μ_w is water viscosity, R is the radius the grout permeates through the soil, and n is porosity. In this equation, the time, length and viscosity are consistent and cancel out, causing K_F to be unitless. Several of these parameters are held constant in this study. For example, grout viscosity, μ_g, was equal to 11 centipoise at a water-to-cement ratio of 2 (Gallagher, 2000), H is 14.1 meters, r is 0.005 meters, R is 0.025 meters, and μ_w is 1 centipoise. The result of the penetration rate versus the permeability factor is shown in Figure 2.12. The data in the figure is representative of four soils with four volumetric water contents, ranging from 0 to 14.4 percent. Relative hydraulic conductivity, used in Equation 15, was found using the Campbell (1974) equation as previously discussed.

The results for the penetration rate versus the effective permeability factor are shown in Figure 2.12. The relationship between penetration rate and the permeability factor is

$$P_R = \alpha_1 K_F^{\alpha_2} \tag{19}$$

where P_R is the penetration rate, K_F is a unitless permeability factor, $\alpha_1 = 0.06$, and $\alpha_2 = 0.4$.

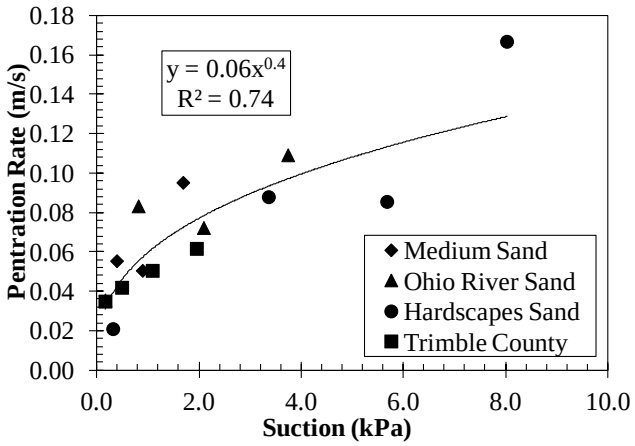

Figure 2.12. Soil Penetration Rate versus Permeability Factor.

As previously discussed, the rate of injection was greater in partially saturated sand than that of dry sand. This is was previously described in Figure 2.10. However, the major influence on the permeability factor was the unsaturated hydraulic conductivity, which was calculated directly from suction values obtained from the SWCC. The trend between penetration rate and the permeability factor existed for several reasons. As the amount of water in a soil was decreased, the soil particles absorbed more of the grout moisture, decreasing the amount of penetration as the suspension propagates through the soil (Perret et al., 2004). Another major factor in this relationship was the suction of the soil, as shown in Figure 2.11. The increasing suction associated with partially saturated soils can cause increased flow rates from dry conditions. This can be physically described from typical unsaturated soil mechanics testing, in a drying curve, where it takes more pressure to extract water from the pore spaces of the soil as moisture decreases. The same observation can be seen in grout flow in unsaturated soils, as sands with more moisture accepted exhibited higher flow rates and drier soils received the grout at lower rates at the same pressure. Another major factor, related to the suction, was the non-continuous arrangement of moisture within the pore spaces of the soil skeleton. Whereas the pore water in saturated soils tend to be replaced by injected grout, the pore water in non-continuous, unsaturated condition mix with the grout, creating an grout-water mixing zone with significantly higher unmixed water-to-cement ratio. This was dissimilar from dry soils, where no water exists, and saturated soils, where a relatively small grout-water mixing zone exists.

2.6 Strength Testing and Analysis

2.6.1 Unconfined Testing

Unconfined compression was used to evaluate the effects of grain size and amount of initial moisture on the strength of grouted sands. Several common standards exist for various types of soils and grouted soils, yet none exist specifically for cement injected soils. However, ASTM D4219 exists for the evaluation of chemical-grouted soils. This ASTM has been used in previous research to assess cement grouted sands (Mollamahmutoglu and Yilmaz, 2011). The stress-strain curves are shown in Figure 2.13.

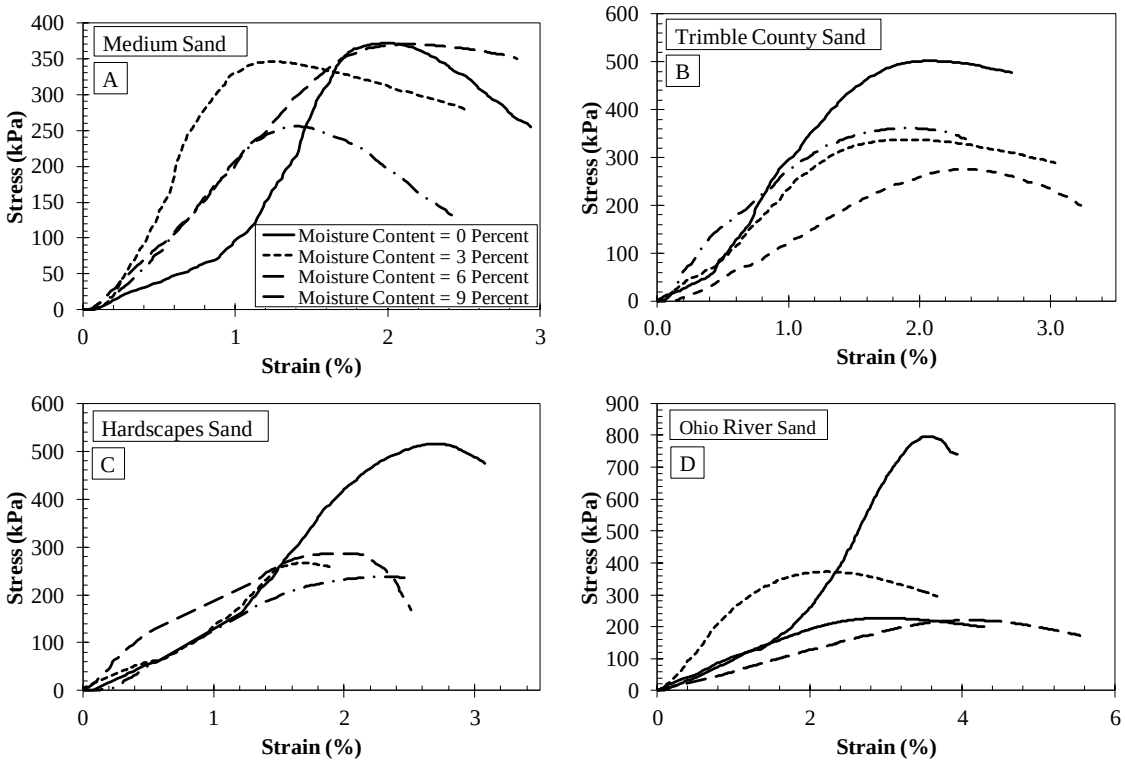

Figure 2.13. Ultrafine Grout Stress-Strain.

In this study, special consideration was taken to ensure adequate strain rates were used in the unconfined compression testing program. However, previous research has shown that strain rates from 0.0125 to 12.5 percent had negligible effect on strength for cement-grouted sands and these finding have had continued usage and verification (Dano et al., 2004; Markou and Droudakis, 2013). The strain rate indicated in ASTM D4219 was used in this study. The strain at peak stress tended to occur roughly at two percent. This was typical behavior for cement grouted sand (Vipulanandan et al., 1994).

2.6.2 Grain Size

This study utilized four different sands to assess the effect of soil properties on the strength of a grouted soil. As previously indicated, ultrafine grouted sand research has been performed in regard to grain size. Markou and Droudakis (2013) used soils with larger particle sizes than what was used in this study. For comparison of strength of various soil gradations, several grain size parameters have been studied. Two common parameters used for comparison of strength is the effective grain size, D_{10}, and the Coefficient of Uniformity, C_u. Ozgurel and Vipulanandan (2005) found that coefficient of uniformity yielded better strength predictions than that of the effective grain size in poorly graded soils. While previous research have been instrumental in showing that grain size has significant implications on strength, only soil specific relationships have been developed. As a result, it is known that grouted sand strength tends to increase as the uniformity of soils gradation increases and decreases with increasing effective grain size (Karol, 2003). While previous research has shown trends with particle size, continuation of this research will be necessary if grouted sand strength estimation will be possible for variations in grain size.

It was hypothesized in this study that the specific surface area, S_s, would show greater correlation to strength than other indices. This was because the specific surface area represents the amount of contact area available in the soil matrix, rather than pertaining to one soil parameter. Strength changes in these data were attributed to the greater about of inter-granular contact for soils with a larger specific surface area. The equation for specific surface area is

$$S_s = \frac{SF}{D_{eff}} \tag{20}$$

where SF is a shape factor, commonly 6 for round-grained soils, and D_{eff} is the effective diameter. The effective diameter is

$$D_{eff} = \frac{100\%}{\sum \frac{\Delta F_i}{\sqrt{D_{max,i} D_{min,i}}}} \tag{21}$$

where $D_{min,i}$ is the minimum grain size for a selected interval, $D_{max,i}$ is the maximum grain size in a selected interval, and ΔF_i is the percentage correspond to the selected grain size interval. The results for strength in regard to specific surface area can be seen in Figure 2.14. This figure shows the trend for normalized compressive strength in respect to specific surface area for various gravimetric moisture contents. The strength data was normalized to the neat grout strength. Normalize compressive strength is

$$q_{u(n)} = \frac{q_{u(gs)}}{q_{u(ng)}} \tag{22}$$

where $q_{u(n)}$ is the normalize unconfined compressive strength, $q_{u(gs)}$ is the grouted sand unconfined compressive strength, and $q_{u(ng)}$ is the neat grout compressive strength. This term was significant because it expressed the variation of the grouted sand from neat grout conditions and the as-mixed grout conditions). It also provides future researchers the ability to compare the data in this study to their normalized data.

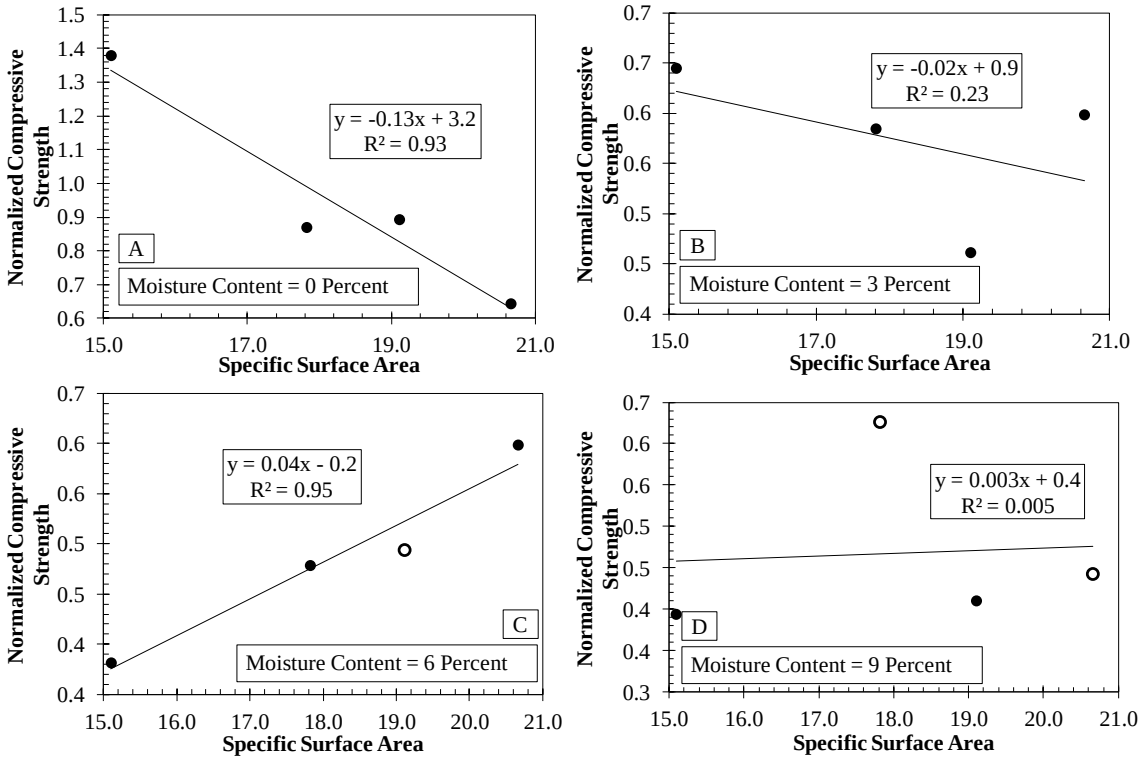

Figure 2.14. Effective of Specific Surface Area on the Unconfined Compressive Strength.

Figure 2.14 has interesting features that are due to several factors. For the zero and three percent moisture content samples, the strength tends to decrease with specific surface area. This was due to the inverse relationship between specific surface area and particle volume (Jury and Horton, 2004). The adsorption in the higher volume, lower specific surface area, samples cause increases in strength (Perret et al., 2004). The particles adsorb water from the cement mix, decreasing the water-to-cement ratio, and increasing strength. The nine percent data did not correlate. This was because the unconfined testing did not satisfy ASTM standards, as they failed at two minutes or less. One sample in the six percent moisture content data also failed this criterion. Adsorption behavior appears not to exist in the six percent moisture content samples, which increase with specific surface area. This strength increase was attributed to the inter-granular forces are increased with more particle interaction with greater particle surface areas. The high data correlation affirms that specific grain size may be a useful tool in the understanding of the effects of grain size on grouted sand strength. These data for samples with zero, six, and nine percent moisture were not included because the data did not exhibit known behavior. The shown trend provides evidence that additional research may provide a relationship between specific grain size and strength.

2.6.3 Volumetric Moisture Content

Typically, grout research has been performed on saturated soils to model behavior below the ground water table. Due to the high interest of strength behavior below the ground water table, the majority of previous research and known behavior has been developed for saturated in situ conditions (Karol, 2003). However, it has been shown that soils exhibiting moisture contents short of saturation behave much differently than saturated soils. In saturated conditions, the soil displaces the initial water in the pore spaces of a soil (Xanthako et al., 1994). In unsaturated conditions, initial water does not get replaced. Instead, it mixes the grout mix and dilutes the grout that settles in the soil pore space. These effects could be detrimental, as grouts become unstable with dilution.

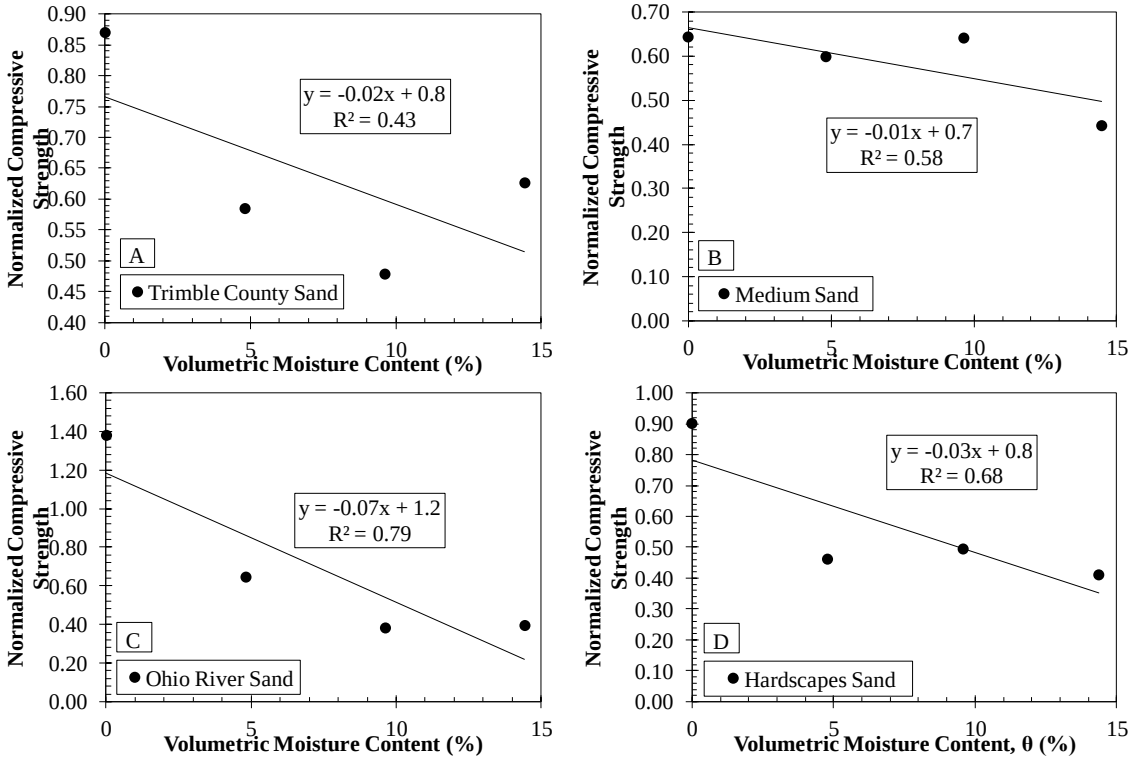

Figure 2.15. Compressive Strength versus Volumetric Moisture Content.

The effects of water on the stability and strength of grout mixes have been previously discussed in this study. In this study, the effect of initial moisture on the resulting strength of grouted sand was investigated. Trends can be seen between volumetric water content and strength in Figure 2.15. Simply analyzing the behavior of the grout based on moisture does not yield relationships that encompass each soil; ergo, investigations into other measures involving the initial soil and grout should provide relationships that encompass multiple soil types and volumetric considerations.

One measure used to evaluate the strength of grouted sands was the volumetric grout ratio, $\Delta V/V_i$. This was the ratio of the grout mix injected into the sample to the components of the grouted sand initially in the sample. Similar volume relationships have been developed for soils that have solidified by means of freezing. This was a ratio of changes volumetric conditions to initial volumetric conditions. Since we know water and soil solids are incompressible, we can assume the two percent strain change occurs in the grout volume. This parameter may also provide insight as it compares the compressible grout component to the incompressible initial components. This parameter is defined as

$$\frac{\Delta V}{V_i} = \frac{V_g}{V_s + V_w} \tag{23}$$

where V_g is the volume of the grout, V_s is the volume of the soil solids, and V_w is the volume of the initial water in the sample. The results of the plot of volumetric moisture content can be found in Figure 2.16. The figure shows a trend as the volume of the grout in the sample increases. D4219 suggests that samples should fail above two minutes. Three samples in this study failed at or below two minutes. These samples have been presented, but have not been included in the relationship. While the data seems to trend with the volumetric grout content, the resulting correlation coefficient was insufficient to suggest a relationship exists. This was likely because the parameters fail to take the different particle sizes into effect. An initial parameter influenced by the moisture, unit weight, and grain size may yield a relationship for the grouted sand strength.

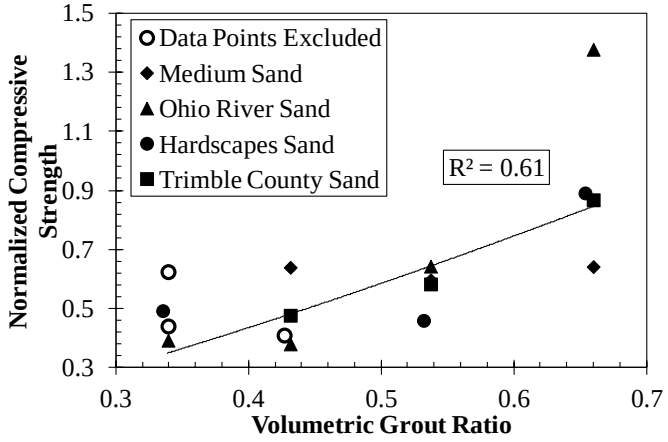

Figure 2.16. Compressive Strength versus Volumetric Grout Ratio.

2.6.4 Unsaturated Soil Mechanics

As previously described, the soil-water characteristics curve relates soil moisture and matric suction. The distinction of the values obtained from the curve was that they are soil-state specific. This becomes a useful parameter for this study, because the grain size parameters vary between the different soils. Soil strength has commonly been investigated directly in comparison to matric suction (Fredlund and Xing, 1994). The reason for this correlation was expected, because the matric suction values obtained from the SWCC are soil-specific and dependent upon the initial moisture in the sample. The

correlation between moisture content and matric suction can be seen in Figure 2.17. Matric suction was normalized to the air entry values specific to each SWCC curve. The same samples have been excluded in Figure 2.17 as were excluded in Figure 2.16. The relationship between normalized unconfined compressive strength and normalized suction is

$$q_{u(n)} = n_1(\psi_n)^{n_2} \tag{24}$$

where ψ_n is the normalized soil suction. The equation for normalized soil suction is

$$\psi_n = \frac{\psi}{\psi_{aev}} \tag{25}$$

where ψ is the matric suction corresponding to the in situ volumetric moisture content and ψ_{aev} was the matric suction air entry value. For the power function constants, $n_1 = 0.9$ and $n_2 = 0.08$. Equation 24 is valid for the initial soil conditions, grout mix, and procedures used in this study. It should be noted, that this was the initial matric suction of the in situ soil, used to predict strength of the resulting grouted sand. This was not the matric suction of the grouted sand sample itself. Additional research will be necessary to continue developing these relationships.

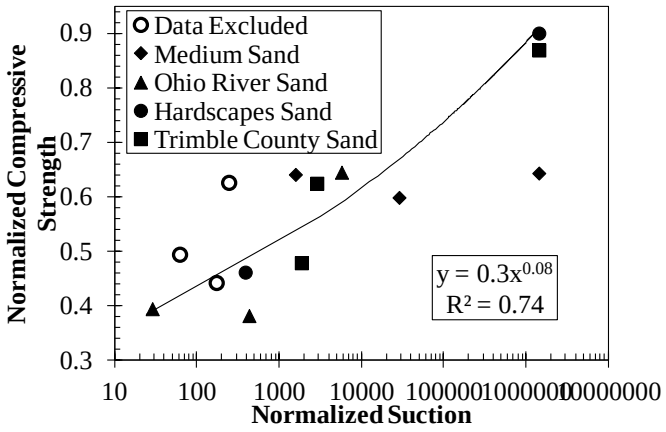

Figure 2.17. Compressive Strength versus Suction.

The power function empirical parameters have significant relevance in this study. Constant, n_1, signifies the normalized compressive strength of the sample when the normalized suction was equivalent to one. The exponential constant of the power

function was positive but below zero. Since this was positive, the strength continually increased with increasing suction. However, since the exponent was below one, the increase of one normalized suction results in a decrease in the rate of increase by a factor of 0.08. This means the strength values will be close to that of dry suction conditions as the initial soil suction approaches that of dry conditions. This was dissimilar to low suction conditions, where small changes in initial suction will significantly affect strength.

2.7 Conclusion

The influence of initial conditions on grouted sand properties, such as moisture content and variation in grain size, were evaluated. The grouted sand properties were investigated how these aspects influences grout penetration into the soil and the resulting grouted sand strength. Also, influent of water-to-cement ratios were investigated in respect to neat grout specimens. The conclusion drawn from this study are as follows:

- Unsaturated hydraulic conductivity increases (ie. from 8.9×10^{-4} cm/s to 2.0×10^{-2}) with changes in graviemtric moisture from zero to nine percent. Matric suction was used to estimate the unsaturated moisture content.
- Increases in water-to-cement ratio have a significant effect on bleed. Increasing the water-to-cement ratio from one to four increased bleed from zero percent to 50 percent, causing the grout to be unstable. Similar changes in the water-to-cement ratio decreased the unconfined compressive strength by a factor of ten.
- As discussed, previous studies have shown that soils with five percent fines can be ungroutable. In this study, fine sand with eleven percent fines was investigated. This particular sand was not groutable. By all groutability criteria, this sand was considered moderately groutable. These results affirm assertions of previous studies that sand considered moderately groutable may not be groutable.
- Grout penetration rates through the sample increased, by as much as a factor of eight, as volumetric moisture increased from dry conditions to nine percent moisture. The observed grout penetration increase was directly related to unsaturated hydraulic conductivity. Relationships regarding injection and soil properties can be used in conjunction with hydraulic conductivity to develop relationships in initial penetration rates.

- Grouted sand strength decreased as moisture increased. A 50 percent decrease in strength was observed with an increase of nine percent gravimetric moisture. This was likely due to mixing of pore water and the grout suspension.
- With greater proportions of grout to initial soil and water, strength increases were seen. As the initial suction increased from about 50 to 1,000,000 kPa, the grouted sand strength increased by 150 percent. The soil-water characteristic curves are dependent upon the unit weight and soil-specific particle sizes. The specific soil suctions were selected from the appropriate initial moisture of the soil. This allows for grouted sand strength relationships based on soil matric suction.

CHAPTER 3

3 Mechanical Behavior of Acrylate-Grouted Sands

3.1 Introduction

3.1.1 Grouting Introduction

Chemical grouts have shown effectiveness for geotechnical engineering solutions where seepage control is needed. In particular, chemical grouts are beneficial for stopping water infiltration into underground structures, such as tunnels and mines. In cured form chemical grouts, due to the low permeability, have also been beneficial in providing sustainable solutions for earthen impoundments in need of mitigation due to high seepage rates. Several studies have been implemented to investigate factors contributing to the modification of soils using chemical grouts. These studied have shown the general efficacy of chemically modified soils, investigated properties of the grout in question, and the effects of initial conditions of the soil in the resulting grouted soil (Vipulanandan and Krizek; 1986; Persoff et al., 1999; Karol, 2003; Ozgurel and Vipulanandan, 2005). As various chemical grouts continue to be used for field applications, investigation concerning the impacts of in situ conditions on penetration of the grout into the soil and the resulting grouted soil strength will be beneficial, if not necessary, for improved grouting techniques and design.

In grouting applications, chemical grouts are implemented where cement-based grouts have demonstrated ineffective results, such as failing to reach target seepage reductions. Situations involving seepage reduction measures, where features such as fine cracks in underground concrete structures, earthen impoundments, such as dams, with fine or silty-sands, and situations requiring extraordinarily low permeability seepage barriers, may likely require chemical grouting. In many projects, the need for chemical grouting may not be realized until target seepage reduction with cementitous grouts has been insufficient. Commonly, the least expensive, higher permeability grout material will be applied first. If target seepage reduction has not been achieved, then more expensive, lower permeability grout material is used (Babcock, 2013b). However, for underground structures and grouting of soils in earthen impoundments, a general understanding of the applicability of various grouts to crack sizes or soil grain sizes has begun to surface

(Karol, 2003; Powers et al., 2007; Henn, 2010). General criteria exists which determines applicability of grout to specific soil hydraulic conductivities. It will continue to be important that the variety of grout properties, along with the effects of initial conditions on grouted soils, is understood so that an appropriate grouting effectiveness measures, such as initial soil conditions and injections methods, can be understood and quantified.

3.1.2 Chemical Grout Properties

Commercially available grouts may be composed of a variety of materials that influence the grout properties. The base chemical responsible for the material reaction can vary. Examples of some of the base chemicals are sodium silicate, colloidal silica, urethane, acrylic, acrylamide, and acrylate. These grouts typically have an accompanying chemical that initiates a chemical reaction. This chemical reaction, when only including these two components, hardens to form a gel. Chemical grouts generally have controllable gel times and very low viscosities, which allows adequate permeation into soil for earthen improvement techniques. In field applications, the major use of these grouts has been to serve as an impermeable seepage control barrier. A secondary benefit is increased stability by increasing strength. It is beneficial to be able to estimate a reasonable rate of grout penetration, extent of penetration, and time of gel when permeation will no longer be possible. The accuracy of such estimation contributes to the determination of whether permeability and strength requirements are achieved. Acrylamide-based solutions have been considered the most successful and effective of chemical grouts; however, these grouts are toxic (Zebovitz et al., 1998). In past decades, acrylamide was removed from the market due to toxicity issues, but has since been reinstated due to increased safety technology and understanding proper handling of the product (Krizek et al., 1992; Ozgurel and Vipulanandan, 2005). Acrylate-based grout products offer a non-toxic alternative to acrylamide, and may be the grout of choice where environmental considerations are critical.

Acrylate grout has a viscosity similar to water and has controllable gel times (ranging from several seconds to twelve hours). In cured form, acrylate grout has a low permeability and adds strength to soil. This type of grout consists of three chemical components combined into two mixing tanks. The first tank, Tank A, contains the

monomer and activator. A monomer is a chemical capable of a chemical reaction, or polymerization. The activator aids in the propagation of the reaction and assists the initiator to form a more quality gel, but does not initiate a reaction. The second tank, Tank B, consists of an initiator. The initiator is responsible for the start of the reaction, by decomposing into free radicals when coming in contact with the monomer. The initiator has often been referred to as a catalyst. For a reaction to take place, the monomer and catalyst must be combined. A typical mix design for the monomer, initiator, and catalyst can be found in Table 3.1. Polymerization is the reaction necessary for the hardening of the grout solutions to occur. Acrylate grout is non-toxic, not reversible, and non-degradable in cured form. The grout has the appropriate properties for use as a chemical grout and acrylate grout's efficacy has been shown in various applications.

Table 3.1. General Mix Design for a Chemical Grout.

TANK A	TANK B
Add 37.8 Liters of Water	Add 37.8 Liters of Water
Add Drum (51.1 L) of Monomer	4.54 kilograms of Catalyst
Add 3.8 Liters of Initiator	Bring to 113.5 Liters with Water
Add 20.8 Liters of Water	

3.1.3 Chemical Grout Studies and Applications

Several case histories and studies investigated acrylate specifically. A study by Han (2004) looked at gel time characteristics of the grout only. This researcher did not investigate any properties of the grout, other than gel times and chemical properties. Krizek et al. (1980) tested various engineering properties of acrylate grouted sand, but did not look at variation in initial conditions of those properties. These studies have demonstrated a need for increased investigation into acrylate grout.

Several case histories have shown successful uses of acrylate-based grouts as acceptable grouting materials for earthen embankments. One of which was a fly ash pond, where a mixture of cement grout and acrylate grout was used to provide seepage control and increase shear strength for the impoundment (Bruce, 1992). Acrylate grout has been utilized to stop seepage in a mining application (ECO, 2014). Also, several texts cite the applicability of acrylate and its acceptance for use as a grouting material (Karol, 2003; Warner, 2004; Powers et al., 2007). As chemical grouts continue to be used for

stabilization, the properties of such grouts should continue to be investigated. For grouting applications that involve earthen impoundments, initial conditions of the soils to become grouted should be extensively examined.

3.2 Testing Materials

3.2.1 Test Sands

3.2.1.1 Index Properties

In this study, several natural and mechanically manufactured sands have been selected. These sands were selected to investigate how various grain size indices affect penetration of the grout into the pore spaces of soil. Various sand types were also selected to investigate strength of grouted sand, after the grout had cured in the pore spaces. These sands were not mechanically modified in the experimentation; however, several of the sands may have been modified prior to obtainment in this study. The specific gravity values, presented in Table 3.2, are typical values for other sands used in chemical grout studies (Delfosse-Ribay et al., 2006). Specific gravity values were obtained in accordance to ASTM D854. The grain-size distribution for the sands selected for use in this study is shown in Figure 3.1.

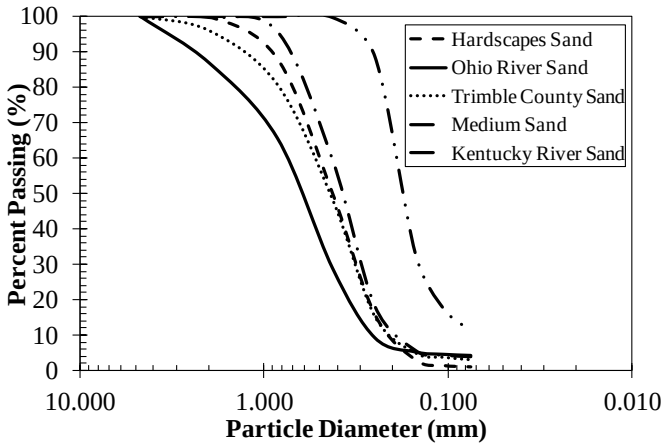

Figure 3.1. Grain Size Distribution.

The five sands investigated in this study were comprised of both natural and mechanically altered sands. Kentucky River sand, Ohio River sand, and Trimble County sand, were obtained from sand mining companies who distribute the sand. These sands are naturally occurring river sands. Two sands, Hardscapes sand and medium sand were manufactured sands. Hardscapes sand was commercially available. Medium sand was

natural sand that was mechanically altered. Relevant properties of these sands can be found in Table 3.2.

Table 3.2. Sand Data.

Sand Name	Specific Gravity, G_s	% Pass #10 Seive	% Pass #10 Seive	% Pass #60 Seive	Fines (%)	Coefficient of Uniformity, C_u
Kentucky River Sand	2.69	0.15	100.0	88.7	11.0	2.5
Ohio River Sand	2.66	0.6	86.85	9.25	4.3	2.0
Hardscapes Sand	2.65	0.41	99.84	15.86	1.0	2.2
Medium Sand	2.66	0.36	99.8	18.2	3.9	2.2
Trimble County Sand	2.66	0.42	95.96	15.22	3.0	2.3

3.2.1.2 Hydraulic Properties

Saturated hydraulic conductivity testing was performed in respect to ASTM D4234. The hydraulic conductivity values obtained in this study was of similar to that of sands in other studies (Anagnostopoulos and Hadjispyrou, 2004; Ozgurel and Vipulanandan, 2005; Bolisetti et al., 2009). The samples in this study had a constant target dry unit weight of 15.7 kN/m^3. The saturated hydraulic conductivities of the soils investigated in the study are shown in Table 3.3.

Table 3.3. Hydraulic Conductivity.

Sand Name	Saturated Hydraulic Conductivity, k_s (cm/s)
Kentucky River Sand	2.5E-04
Ohio River Sand	4.4E-02
Hardscapes Sand	3.5E-02
Medium Sand	2.6E-02
Trimble County Sand	3.8E-02

Due to variability of in situ moisture content in field applications, unsaturated soil mechanics was investigated. A fundamental principle of unsaturated soils is that the soils exhibit suction due to partial saturation. Unsaturated soil mechanics may provide insight into penetration rates, during the grout injection phase of the experiment, in soils that vary from saturated conditions. The phenomena of changes in soil hydraulic properties with changes in moisture moisture have previously been analyzed and the theory has

been presented. Unsaturated soils are also expected to influence grout penetrability and strength of the grouted soil.

3.2.1.3 Soil-Water Characteristics Curves

The soil-water characteristic curve (SWCC) found in this study is shown in Figure 3.2. The SWCC was used to investigate the initial soil moisture for this study. Unsaturated soil mechanics may be a beneficial consideration where grouting takes place in unsaturated soils that are encountered above the water table. The SWCC in the figure were obtained using a parameter optimization method, proposed by Fredlund and Xing (1994).

The value typical for quantifying moisture to formulate equations used for SWCC analysis is the volumetric water content. The volumetric water content can be easily be obtained using degree of saturation, S, and porosity, n; two common parameters used in engineering practice. The equation for volumetric moisture content is

$$\theta = \frac{S}{n} \tag{18}$$

for the volumetric water content. For the optimization procedure, proposed by Fredlund and Xing (1994), is

$$\theta = C(\psi)\left[\frac{\theta_s}{\left\{\ln\left[e+\left(\frac{\psi}{a}\right)^n\right]\right\}^m}\right] \tag{19}$$

where θ is volumetric water content, θ_s is volumetric water content at saturation, and e is 2.718. There are also several variables obtained from the methods. These are fitting parameters a, n, and m. These can be found in Table 3.4

A second equation is needed for correction of Equation 19. This function is

$$C(\psi) = 1 - \frac{\ln\left(1+\frac{\psi}{\psi_r}\right)}{\ln\left(1+\frac{\psi_d}{\psi_r}\right)} \tag{20}$$

where ψ is matric suction, ψ_r is the residual matric suction, and ψ_d is dry matric suction. The dry suction, ψ_d, was a constant, and is 1,000,000 kPa. The last step in the procedure was using Microsoft equation solver to solve the solution. These solutions are non-unique and are material dependent.

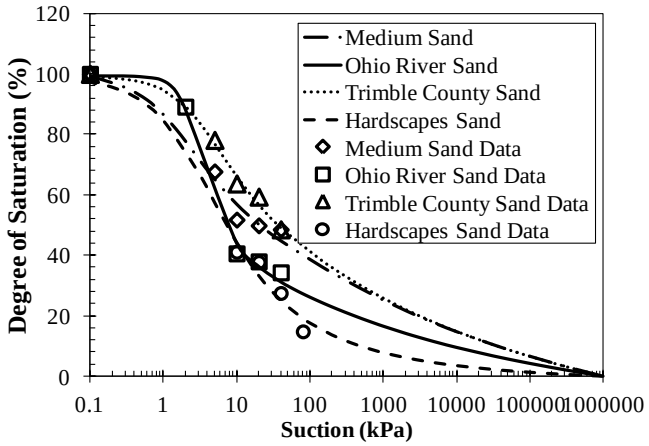

Figure 3.2. Fredlund and Xing (1994) Optimized Fit for Test Sand.

It is known that finer soils have lower hydraulic conductivities. This can be observed in the Kentucky River sand, which had the finest grain sizes and also the lowest hydraulic conductivity. This is attributed to smaller pore spaces for water to travel through in finer soils. In particular, Zapata (1999) showed that the Fredlund and Xing (1994) a-parameter correlated with D_{60}. In this study, the data also correlated with "a". A relationship between "a" and D_{50} can be found in Figure 3.3. Mean grain size, D_{50}, was used because it is a more commonly used parameter. The linear relationship proposed in the figure is

$$a = k_1 D_{50} + k_2 \tag{21}$$

where D_{50} is the median grain size. Parameters k_1 and k_2 are equal to -6.8 and 5.1. The residual suction, ψr, was held constant at 100 kPa for coarse grain graded soils, as suggest by the Fredlund (1999) for initial conditions. Fitting parameters "a", "n", and "m" were bound between 1 to 15150, 1 to 20, and 0.5 to 4, as recommended by Fredlund and Xing (1994). The data for the SWCC curves can be found in Table 3.4.

Table 3.4. SWCC Data.

Sand Name	Saturated Volumetric Water Content, θ (%)	Air Entry Value, ψ_{aev} (kPa)	Fitting Parameter, a	Fitting Parameter, n	Fitting Parameter, m
Medium Sand	39.8	0.7	1.0	1.2	0.5
Ohio River Sand	39.8	1.4	2.1	3.2	0.5
Trimble County Sand	39.8	1.4	2.6	1.4	0.5
Hardscapes Sand	39.5	13	2.6	1.0	1.3

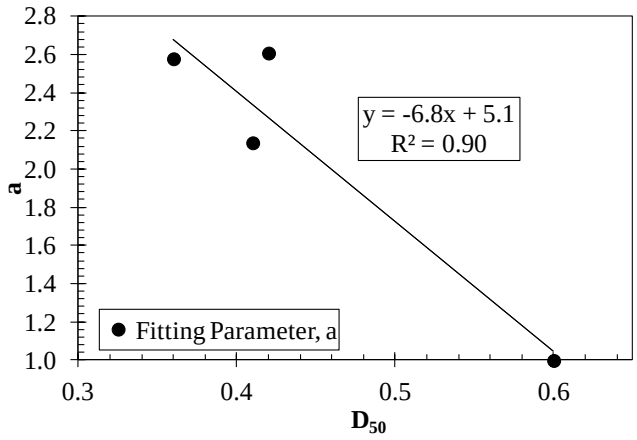

Figure 3.3. Fitting Parameter "a" versus D_{50}.

3.2.1.4 Hydraulic Conductivity of Unsaturated Soils

In geotechnical engineering, saturated hydraulic conductivity have been used for seepage considerations. However, hydraulic conductivity is also dependent on the soil moisture state (Fredlund et al., 2012). In order to estimate a quantification of the change in hydraulic conductivity due to moisture, a unitless parameter called relative hydraulic conductivity has often been used. Relative hydraulic conductivity is defined as

$$k_r = \frac{k_w}{k_s} \tag{22}$$

where k_w is the unsaturated hydraulic conductivity and k_s is the saturated hydraulic conductivity. Figure 3.4 shows relative hydraulic conductivity versus degree of saturation.

Fredlund (2006) presented numerous methods for estimating hydraulic conductivity. One in particular was selected for used in this study, is the Campbell (1974) relationship, which is a power function defined as

$$k_r = (\psi_n)^{-4/b} \tag{23}$$

where k_r is relative hydraulic conductivity, b is a constant, and ψ_n is normalized suction. In Equation 23, b = ln(ψ_0). This equation is reasonable for engineering practice (Fredlund, 2006). Suction at dry conditions, ψ_0, is 1000000 kPa. Normalized suction is a unitless parameter defined as

$$\psi_n = \frac{\psi}{\psi_{aev}} \tag{24}$$

where ψ_{aev} is the air entry value and ψ is the suction at a corresponding volumetric water content selected from the SWCC. The air entry values, along with other relevant parameters and values, can be found in Table 3.4.

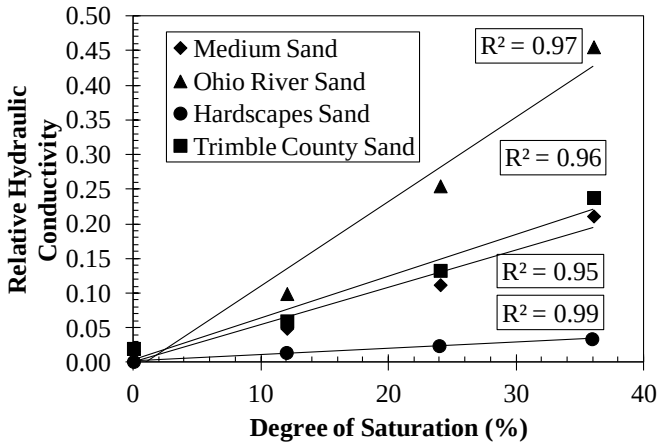

Figure 3.4. Relative Hydraulic Conductivity versus Volumetric Moisture Content.

3.2.2 Acrylate Grout

3.2.2.1 Grout Properties

In a polymer reaction, two chemicals combine initiating a free radical polymerization reaction, causing a series of long molecular chains to bond together continuously, resulting in a polymer gel. The stages in this exothermic reaction are initiation, propagation, and termination (Han, 2004). Initiation was the point where the first free radical attaches to the first monomer particle. The chain reaction continues as free radicals continue to combine with the monomer. This is called propagation. As propagation continues the reaction comes to the point where the free radicals terminate

and the molecular monomer chain reaction stops. This is called termination. The process is an exothermic reaction, meaning heat was a byproduct of the reaction. By definition of the reaction stages, the propagation phase will be accompanied by temperature increase. Upon termination, the temperature will begin to decrease because free radicals are no longer creating reactions with the monomer molecules. Figure 3.5 shows a typical temperature-time reaction curve for polymer grouts, with the polymerization stages labeled.

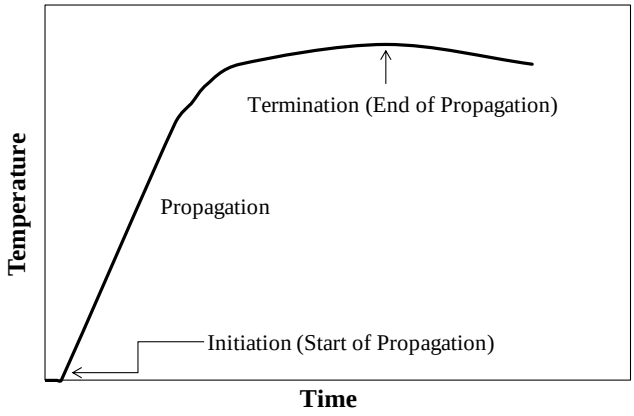

Figure 3.5. Typical Temperature-Time Reaction for Polymerization Reactions.

3.2.2.2 Mix Design

The acrylate grout used in this study, provided by Avanti International, has two primary components: a monomer and a catalyst. The trade name of the base chemical for this study is AV-160 Supergel, which a magnesium acrylate based grout. The viscosity of the grout can be as low as 1-2 centipoise, compared to 1 centipoise for water. The low viscosity makes this grout ideal for pressurization and injection into fine pore spaces. Acrylate grout has an orange tint in uncured form. In cured form the permeability can be at low as 10^{-8} cm/s and exhibits strengths of 827 kPa in sand (Avanti International, 2014A). A component premixed with AV-160, prior to mixing with the catalyst, was the AV-101 Catalyst T^{+}, an activator. This clear liquid was pre-mixed with the catalyst, with water, in equal proportions to the catalyst in Tank A. The catalyst used in this study was AV-103 Catalyst SP, which was the initiator in the reaction. The catalyst was composed of sodium persulfate. Acrylate can be catalyzed by ammonium persulfate or sodium persulfate. Sodium persulfate was chosen for this study because it has less oxidation

potential than ammonium persulfate, and the lowest hazard products were chosen for this study. AV-103 was mixed in another tank, Tank B. As previously stated, the activator, AV-101, and the initiator, AV-103, must be mixed in equal proportions. The typical concentration range for the activator and inhibitor, each, is one to three percent. When percentages are referred to in solutions, this pertains to a measurement of the part of the chemical component to 100 parts of the total solution. For example, this can be measured and reported as the mass in grams granular, chemical component to 100 milliliters of the total solution. A two percent catalyst solution was chosen for this study, as the median percentage recommended by Avanti's product sheets. In Table 3.5 a typical mix design used in the field can be seen. This design gives a two percent catalyst mix with no additives. However, in chemical grouting applications longer gel times are necessary to allow grout to permeate through the soil. There are several ways to elongate the time of reaction upon mixing, allowing longer gel times for pumping and permeation of the grout through the soil.

Table 3.5. Typical Mix Design for Acrylate Grout, AV-160, with no KFe.

TANK A	TANK B
Add 37.8 Liters of Water	Add 37.8 Liters of Water
Add Drum (51.1 L) of AV-160	4.54 kilograms of AV-103
Add 3.8 Liters of AV-101	Bring to 113.5 Liters with Water
Add 20.8 Liters of Water	

3.2.2.3 Grout Gel Testing

There are several factors that affect chemical grout gel. The initial conditions of the uncured grout, such as dilution and catalyst concentration, severely alter the gel time. However, controlled water volumes and catalyst concentrations are easily achievable. While the mix design may be used to control gel, daily changes in temperature can be a major obstacle for gel time control in field grouting.

In the exothermic reaction, excess heat was given off from the reaction change from liquid to semi-solid. Therefore, the maximum curing temperature has a direct correlation to the gel time. Therefore, ambient temperature is a major external condition that has been shown to alter the maximum curing temperature. As the initial grout temperature was changed, the final temperature and cure time was effected. Temperature may

potentially be managed by putting bags of ice in the grout when the temperature becomes hot and by add warm water to the mix when the external temperature becomes cold. Gel times may be managed by temperature control and catalyst control, but with these there are limitations to the length of extension.

By varying parameters such as catalyst concentrations, maximum gel times of several minutes can be achieved. Grouting text books and case studies indicate that extended gel times are necessary for geotechnical applications (American Cyanide, 1960; Nonveiller, 1989; Bell, 1993; Bruce et al., 1997; Karol, 2003). Potassium Ferricyanide (KFe) is a chemical compound used in small quantities for extending gel times in chemical reactions, as much as several hours. KFe acts a reducing agent that retards free radical generation, necessary to start the reaction (Avanti International, 2014B).

In this study, four KFe concentrations were tested at three different temperatures. Figure 3.6 shows the temperature changes with time as an acrylate polymerization exothermic reaction progresses. In this figure both temperature and time were normalized. Normalized time is

$$t_n = \frac{t}{t_{max}} \tag{25}$$

where t the time and t_{max} is the time corresponding to the maximum temperature, also known as curing temperature. Normalize temperature is

$$T_n = \frac{T}{T_0} \tag{26}$$

where T is temperature, in degrees Celcius, and T_0 is ambient temperature. As previously mentioned, KFe extends gel times by retarding free radical generation. Free radicals are necessary for the reaction to initiate.

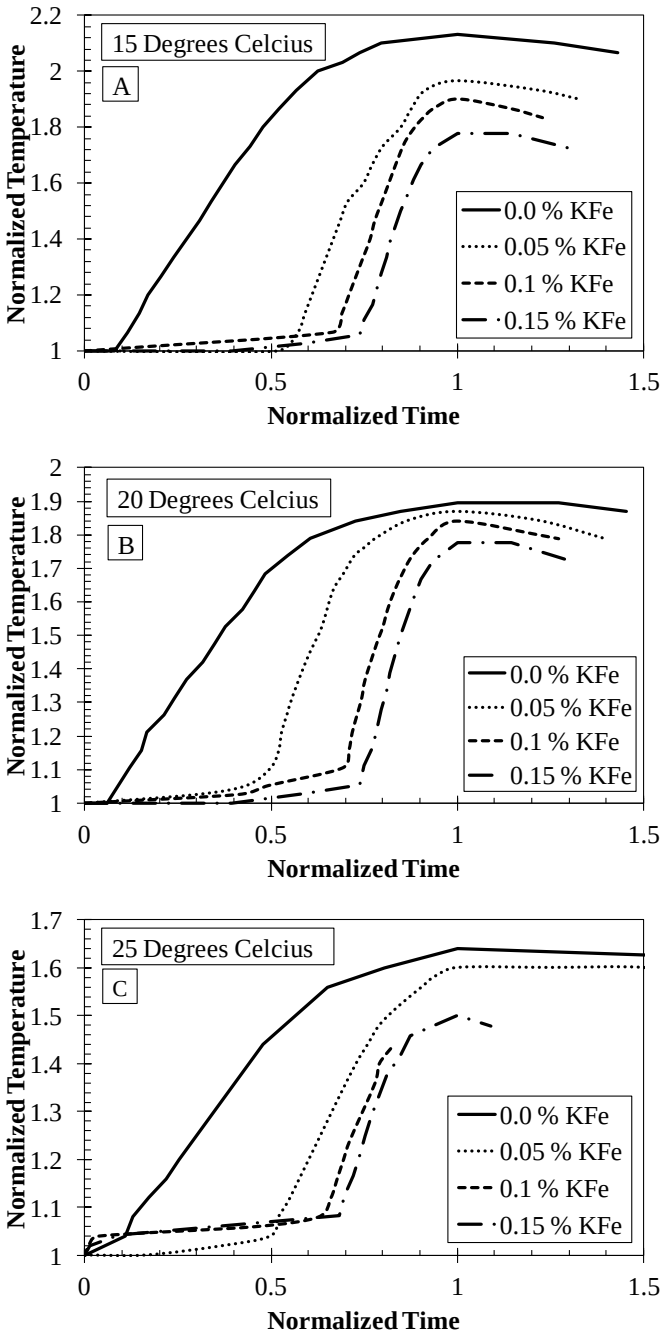

Figure 3.6. Time-Temperature Curve during Acrylate Polymerization.

In Figure 3.6, it was apparent that as more KFe is added to the solution the point of initiation was prolonged. Also apparent in the figure, samples with larger proportions of KFe exhibit lower maximum temperatures. This may be because some free radicals are lost as KFe retards free radical general. Curing Temperature variations can also be seen in Figure 3.7.

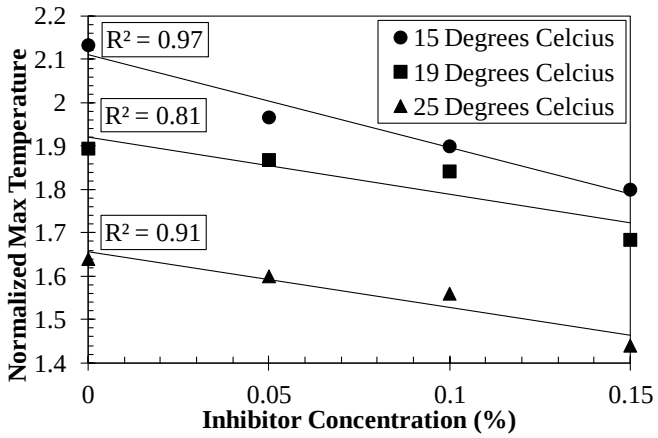

Figure 3.7. Normalized Maximum Temperature versus Inhibitor Concentration

The inhibitor chemical, KFe, extends the time for reaction initiation by retarding monomer free radicals, which results in a decreased temperature. The maximum reaction temperature was normalized by the ambient temperature for analysis in this study. The associated ambient temperature has been presented in the data label, seen in Figure 3.7. The equation for normalized maximum temperature time is

$$T_{n,m} = \frac{T_{max}}{T_0} \tag{27}$$

where T_{max} is the maximum temperature and T_0 is the ambient temperature. The samples tested at 15 degrees Celsius have the highest increase in temperature from ambient temperature, but display the lowest temperature overall. The opposite was true for the samples tested at 25 degrees Celsius.

While the samples tested at lower ambient temperature had higher normalized maximum temperature, the samples tested at higher ambient temperature reached the higher maximum temperatures overall. The samples that reached the highest maximum temperatures had faster gel times. Figure 3.8 shows the effect of KFe on gel time of the grout. Gel time of the acrylate grout was quantified as the time where the grout became sticky enough to stick to a stirring rod, forming a string at the end of the stirring rod rather than a droplet (Krizek, 1992). This gel time method was indicative of changes in grout properties (ie. stickiness) and viscosity increases.

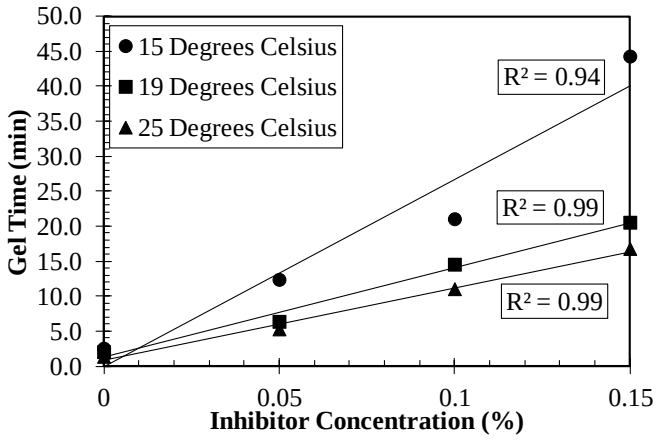

Figure 3.8. Effect of Inhibitor (KFe) Concentration on A) Gel Time and B) Maximum Temperature.

Gel time was of particular importance for a variety of reasons. One imminent reason was for the preservation of equipment. Imperative in the field and in this laboratory study was that the gel does not react in the mixing tank, potentially forming a gel and damaging equipment. Furthermore, gel time has a crucial role in the effectiveness of the grouting program. In field grouting, grouting typically takes place by drilling vertically into the ground, inserting an injection sourced into the drilling hole, and injecting grout laterally while pulling the injection source to the ground surface. For the flow from the injection source, the length that the grout is able to penetrate from the center of the injection source is called the grout radius of penetration. For a grouting program to be effective, the grout must be able to permeate through the soil to achieve the designed grouted sand radius. If the grout gels before penetrating the appropriate radius, the seepage barrier may be non-continuous. This may cause mechanical instability and potential areas for water flow to bypass the seepage barrier. For controlling gel time the inhibitor, potassium ferricyanide, was added to achieve the proper gel time.

Selection of a mix design for controlling gel times varies by application and specific grout design. In chemical grouting for grout curtain applications, several textbooks have proposed that ranges from 15 minutes to several hours may be acceptable (Bell, 1993; Bruce et al., 1997). Case history data has been presented that verifies these ranges are appropriate in field grout curtain applications (American Cyanide, 1960; Nonveiller, 1989; Karol, 2003). For the purpose of this study, a potassium ferricyanide concentration

of 0.15 percent was selected, with a gel times of 20.5 minutes. The mix design selected for this grouting program is shown in Table 3.6. It should be noted that more water was added, to Tank A, than shown in Table 3.5. Table 3.5 shows a typical mix design for acrylate grout per Avanti's Technical Data sheet. Table 3.6 shows a mix design that was provided with the grouting material, along with the amount of KFe to obtain the desired gel time for this study. This gel time itself was acceptable because it fits in the range used in field applications of chemical grouting for grout curtains.

Table 3.6. Mix Design for Prepared Grouted sand Specimens in this Study

TANK A	TANK B
Add 37.8 Liters of Water	Add 37.8 Liters of Water
Add Drum (51.1 L) of AV-160	4.54 kilograms of AV-103
Add 3.8 Liters of AV-101	Bring to 113.5 Liters with Water
Add 20.8 Liters of Water	
0.34 kilograms of KFe	

3.3 Grouting Apparatus

In grouting applications, the grout must permeate through the pore spaces of the soil in question, distributing a uniform mix to the pore spaces. Laboratory techniques must mimic such procedures in order to be applicable to field samples. Therefore, the apparatus used in the procedure was developed with the field application in mind. In order to execute the creation of such an apparatus, previous studies were investigated to supplement applicable standards, such as ASTM D4320. The apparatus is shown in Figure 3.9. Any variations from pertinent ASTMs will be noted.

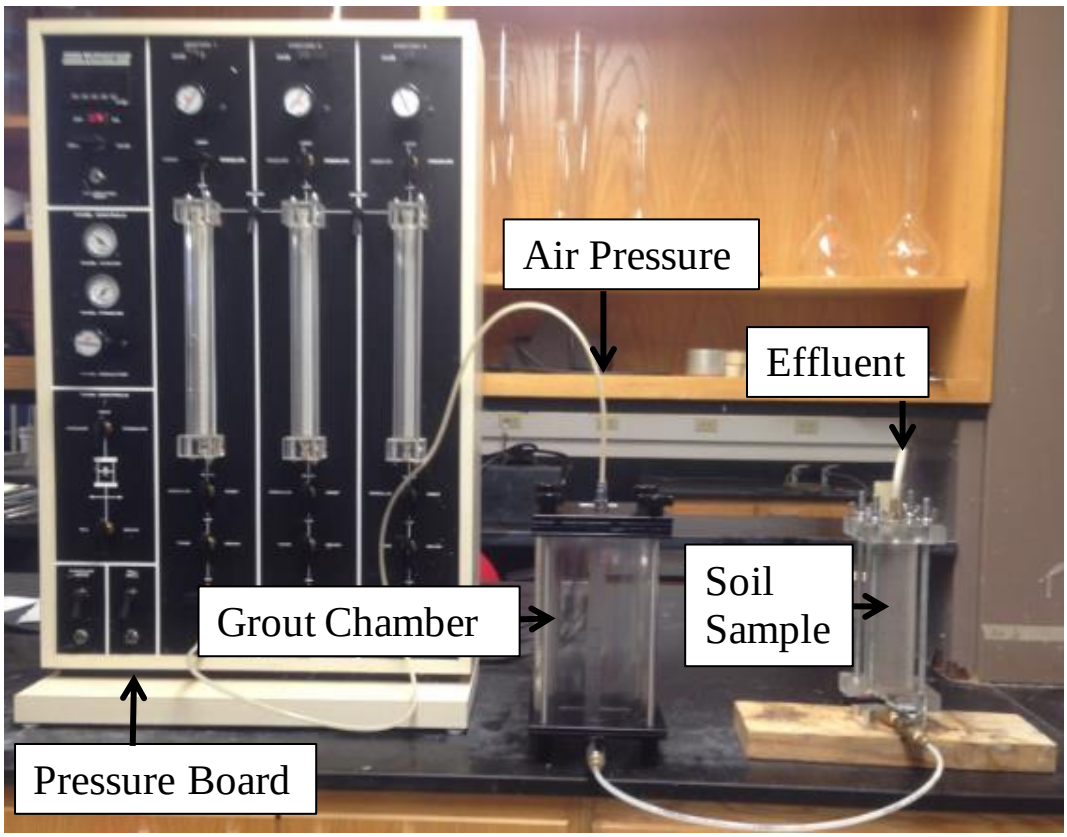

Figure 3.9. Grouting Apparatus.

A major component of the study was that a cylindrical column, for the soils sample, was formed so that the grout could permeate through the porous medium. For this procedure to occur the grout must not leak and the sample soil particles should be stationary through the grouting process. The soil should be stationary so permeation may take place in the soil pore space, without significantly altering the soil skeleton. A 50.8 diameter, 201.6 long acrylic tube was used for the cylindrical mold. The soil sample length was 196.8 millimeters, because the mold fit 3.2 millimeters into the influent and effluent bases, where O-rings were located for leakage prevention. These bases were located at the bottom and top of the sample, and were made from acrylic sheet.

No compaction was needed for the Ohio River Sand, Trimble County Sand, and Hardscapes Sand qat dry conditions. Ten tamps were required for the Medium Sand at dry conditions, in four layers. Moist samples were made, and specifically were compacted at three, six, and nine percent moisture. Ohio River Sand, Trimble County Sand, and Medium Sand ten tamps were required each layer for three layers. In the

Medium Sand, eight layers was required with twenty tamps each layer. In addition to the tamping, twenty taps on the side of the mold were required on every other layer. The tamping rod had a weight of 9.9 Newtons. The sand samples throughout this study were compacted at constant unit weight of 15.7 kN/m^3.

Paper filters were placed at the influent prior to compaction. A wire mesh and filter were situated between the sample and effluent after compaction. The wire mesh was required in the effluent to keep the paper filter from breaking. Also prior to compaction, wax paper was situated around the soil sample, to reduce side friction upon extraction of the sample once it was grouted.

Upon proper compaction and assembling of the mold containing the soil sample, the grouting process was allowed to initiate. An influent air pressure was situated at the top of the grout chamber, extending from the pressure board, as depicted. The grout chamber was a DurhamGeo 152.4 millimeter permeameter. Once the appropriate air pressure magnitude was reached a two-way valve, at the bottom of the grout chamber, was opened. This initiated pressurization of the grout. The grout near-instantaneously began to permeate the soil sample. The grout was allowed to flow to 50 milliliters or until refusal. The grouted sample was paced between two rubber mats to cure, roughly 24 ± 6 hours and extracted using a hydraulic press. The sample was then placed in a Ziplok bag, in accordance with associated ASTM standards previously noted. Upon seven day curing the sample was tested.

3.4 Hydraulic Characteristics

3.4.1 Groutability

Hydraulic conductivity gives strong indications of groutability. Several tests have presented conductivity criterion, commonly applied to chemical grouts (Karol, 2003; Powers et al., 2007: Henn, 2010). Powers et al. (2007) considers soils with hydraulic conductivities between 10^{-1} to 10^{-3} cm/s groutable. Soils with hydraulic conductivities between 10^{-3} and 10^{-5} cm/s are considered marginally groutable. Soils that have hydraulic conductivities lower than 10^{-5} cm/s are typically not groutable. The hydraulic conductivity criterion in graphically depicted in Figure 3.10, and these associated data is presented.

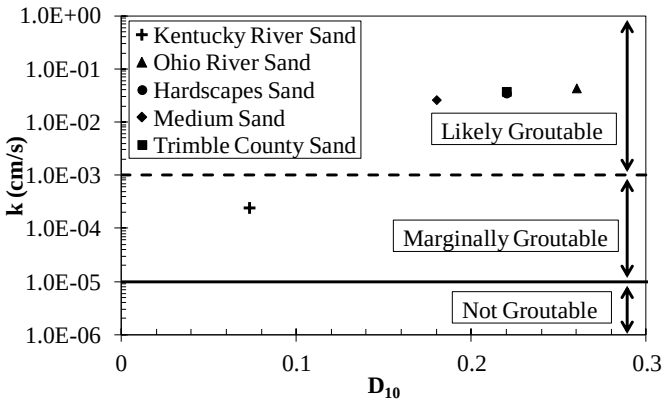

Figure 3.10. Hydraulic Conductivity Groutability Criterion.

By these criteria Kentucky River Sand has a designation of marginally groutable, as its saturated hydraulic conductivity was between of 10^{-3} and 10^{-5} cm/s, while the remaining sands are groutable based on this criterion. This can be observed in Figure 3.10, where Kentucky River sand lies in the marginally groutable region. Once the groutability of the sands was determined, injection of the groutable sands was initiated.

3.4.2 Grout Penetration

Grout penetration was measured in this study. This was considered the time the grout penetrated the cylindrical soil sample, influent to effluent. An important factor in grouting effectiveness in the field is the radius of penetration, which is directly affected by the grout penetration of the soil (Xanthakos et al., 1994). As can be seen in Figure 3.11, grout penetration increased as the soil moisture was increased. Field variation of grout penetration with initial moisture has been noted in a study on cement grout by Perret et al. (2000). One reason for this behavior is adsorption in dry soils. In a dry sand sample, dry particles adsorbed water, which impeded penetration. In soils where these particles contain water, less adsorption takes place and the liquid flowed through the pore spaces freely. Increases in partial saturation increased the penetration rate.

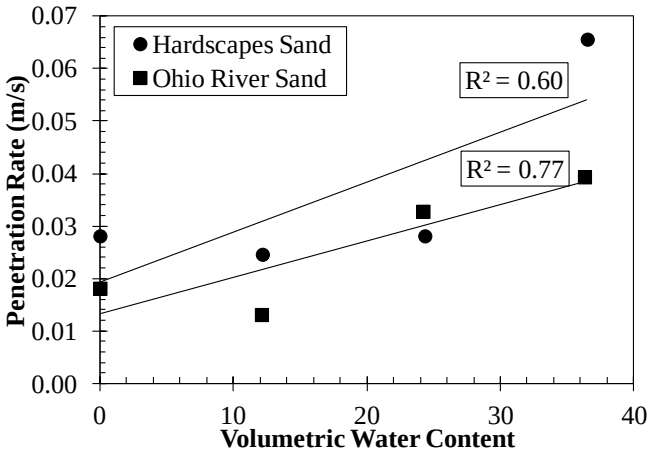

Figure 3.11. Effect of the Degree of Saturation on Grout Penetration Rate.

A common tool used to interpret behavior in unsaturated soils is the soil water characteristics curve, as previously discussed. The penetration relationships, seen in Figure 3.11, can also be understood by sample obtainment processes used to obtain SWCC data. In SWCC testing, as the sample becomes less saturated it takes more pressure to get the remaining water out of the sample, due to the suction of the soil. This relationship for unsaturated soils is applicable to the grout penetration rates observed in Figure 3.11. This was because as the soil moisture content decreased, penetration rates through the sample decreased. While four groutable sands were used in this study, complete penetration rate data was only obtained for Ohio River sand and Hardscapes Sand. Penetration data was obtained for Medium sand and Trimble County sand, but insufficient data was available to suggest trends for these sands.

As previously noted, grout penetration in the field is emitted from an injection source, and penetrates laterally from the point of injection (Xanthakos et al., 1994). Early grout research realized and quantified the necessary hydraulic head to grout soils based on soil hydraulic conductivity, grout viscosity, injection source diameter, and desired grout penetration radius (Raffle and Greenwood, 1961). Flow through a porous media has been theorized using Darcian and Newtonian theory, as applicable for chemical grouts. A relationship previously proposed by Maag (1938) was used in conjunction with previous theory and relationships to add a porosity equation. The resulting equation is

$$t = \frac{\mu n}{3kHr} V_g \tag{28}$$

where μ is grout viscosity, n is porosity, k is the hydraulic conductivity, H is the hydraulic head, r is the injection radius, and V_g is a volume term representing the volume to be grouted. For field applications in Equation 28, the volumetric parameter is

$$V_g = R^3 - r^3 \tag{29}$$

where R is the grout penetration radius, whereas in this study, the volume to be grouted is

$$V_g = LR^2\pi \tag{30}$$

where R is the sample radius and L is the sample length. In this study, grout permeates from an injection source into a cylindrical column, which will result in changes in volumes used in the equations. This study chose to develop a parameter based on known criteria that effects grouting flow. This equation isolated all terms on one side, except the length and time. The resulting parameter, which was the result of the combination of terms other than length and time, is

$$K_F = \frac{k_r H r}{\mu_r \pi R^2 n} \tag{31}$$

where k_r is relative hydraulic conductivity, H is pressure head, r is the injection radius, μ_r is grout viscosity, R is the radius the grout permeates through the soil, and n is porosity. As previously discussed, relative hydraulic conductivity is the unsaturated hydraulic conductivity normalized by saturated hydraulic conductivity. The unsaturated hydraulic conductivity is a function of the suction values selected using the SWCC and the in situ degree of saturation. With the appropriate suction, unsaturated hydraulic conductivity was calculated using the equation proposed by Campbell (1974). In this equation, the units cancel out, causing K_F to be unitless. In Equation 31, the relative viscosity is

$$\mu_r = \frac{u_g}{u_w} \tag{32}$$

where μ_g is grout viscosity and μ_w is the water viscosity. Several of these parameters are held constant in this study. These parameters are r = 0.005 meters, R = 0.025 meters, μ_g = 1 centipoise, and μ_w = 1 centipoise. Length and time were not included in the permeability factor, Equation 31, because these were the parameters recorded in the

experimentation. The graphical results of the permeability factor and penetration rate can be found in Figure 3.12.

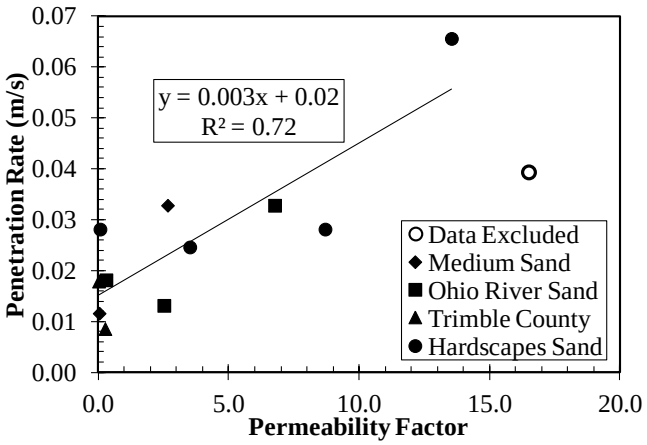

Figure 3.12. Effect of the Permeability Factor on Penetration Rate.

An empirical relationship was developed for the created parameter and flow. This relationship is

$$P_R = \beta_1 K_F + \beta_2 \tag{33}$$

where P_R is the penetration rate, K_F is a unitless permeability factor, $\alpha_1 = 0.003$, and $\alpha_2 = 0.02$.

The slope in the relationship signifies a change in penetration rate per change in permeability factor. The y-intercept was indicative of behavior for dry samples. In this study, a major influent was the calculated unsaturated hydraulic conductivity. Unsaturated hydraulic conductivity was calculated using the Campbell (1974) equation as previously described. This equation used suction and the air entry value, obtained from the SWCC, to estimate unsaturated hydraulic conductivity. Unsaturated hydraulic conductivity was dependent on the soil unit weight, moisture, and grain size. While this factor combines components of these initial conditions, along with associated injection parameters, specific variations in this are responsible for the observed behavior. The major variation was moisture. The lowest permeability factor, indicative of dry samples with low hydraulic conductivity, had low penetration rates due to adsorption (Perret et al., 2000). In the samples with higher permeability factors, the grout penetrated at higher

rates due to higher hydraulic conductivity. Also, there was less air volume for the grout to fill in the pore space, because the water takes up a portion of the pore volume.

3.5 Strength Testing and Analysis

3.5.1 Unconfined Compression

The samples were tested in unconfined compression at a rate of 1 mm/min. The testing machine was allowed to run until failure or until a minimum of twenty percent strain, depending on which occurred first. These tests were performed in accordance to ASTM D5219. Four sands at four different moisture contents were prepared. However, two of the grouted-samples were unstable for testing. Figure 3.13 shows the results of the unconfined compression tests.

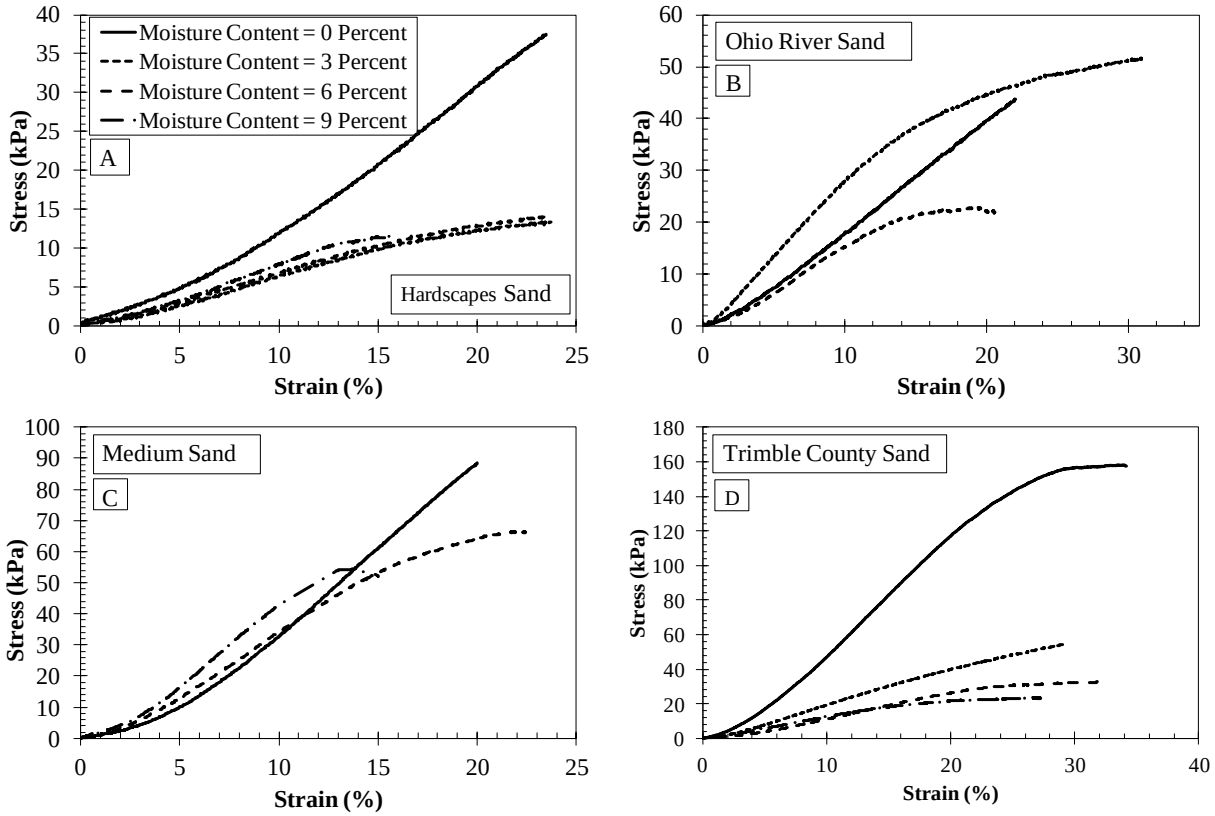

Figure 3.13. Acrylate Grouted sand Stress-Strain Curves.

3.5.2 Relationships

It has been shown in previous studies that grain size has a significant effect on the strength of chemically grouted sands (Schiffman and Wilson 1958; Clough et al. 1979; Christopher et al. 1989). Ozgurel and Vipulanandan (2005) developed an equation to that

empirically gave indication of strength change with grain size and looked at the effects of variation in fines on strength. Common indices of grain size that have been used to evaluate grouted sands are based on grain size and coefficients that give an indication of the soils gradation. While these data does not yield significant correlations, trends in behavior for the grain size of grouted sands can be observed. Further investigation into such relationships should continue to be developed where natural sands are investigated. Furthermore, no data presently exists in regard to initial conditions, such as grain size, for acrylate. Trends between strength and fines content may be observed in Figure 3.14. It should be noted in these results the fines were not incrementally added to one sand. The amount of fines in three natural sands and one manufactured sand was observed. These sands varied in regard to other grain size indices, yet the most apparent observed relationship was in regard to fines content. It should be noted that several of the samples were grouted at variable injection pressures. These samples were included in this figure, but may be omitted in later figures. More research will be necessary to relate grain size properties to strength, and to quantify the role of fines in strength of chemical grouted sands.

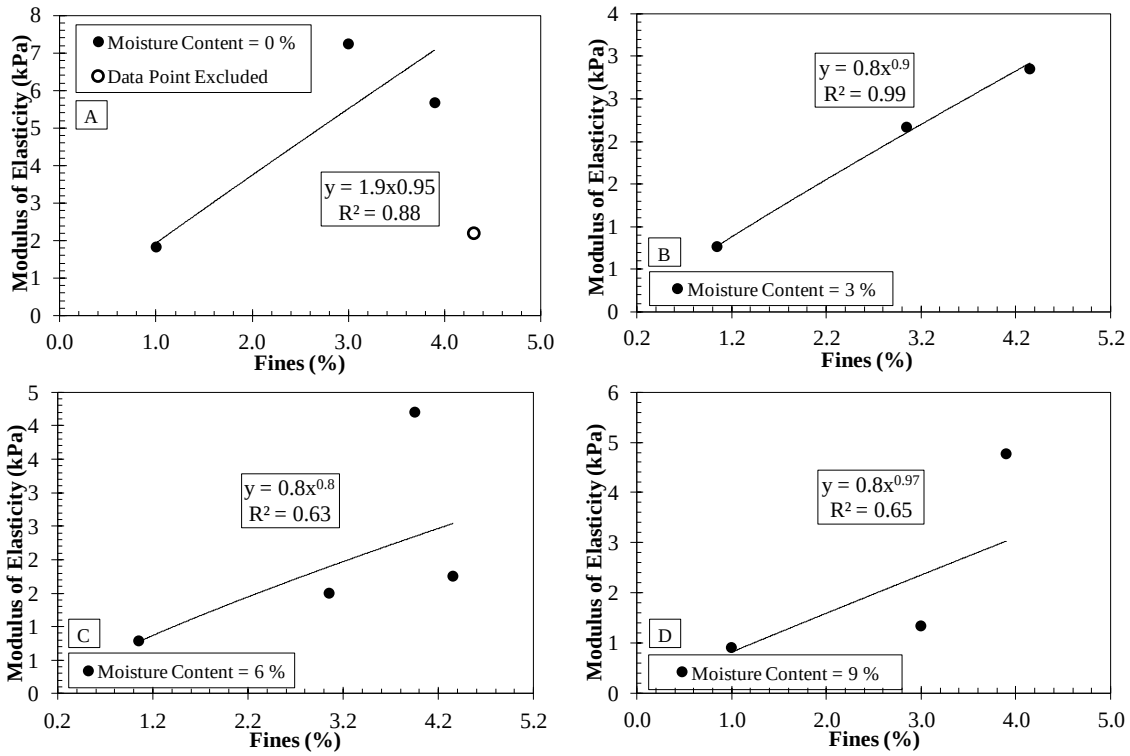

Figure 3.14. Effect of Fines on the Grouted sand Compressive Strength.

Figure 3.14 verifies previous research, that increasing fines content, in this range of fines, increased the grouted sand strength (Ozgurel and Vipulanandan, 2005). In the zero moisture content data set, a sample was excluded because some of the sample was lost through the effluent, as the effluent filter paper broke.

Figure 3.15 shows the direct correlation between soil suction and its effect on strength. The figure shows an increase in strength with suction. Increases in strength with suction, in the figure, were influenced by dilution of the grout upon entering the sample in the low suction samples. This is because low suction soils contain the most water. However, other factors also influenced the grouted sand strength. It should be noted that in the Ohio River sand data the dry sample, having a suction of 1,000,000 kPa, is responsible for the poor correlation coefficient in Figure 3.15B. In this sample, the filter paper broke at the top of the sample. This allowed soil to flow from the sample and is responsible for the poor strength correlation for the Ohio River sand data. All other samples in this study had a wire screen attached, above the filter paper, which further prevented this from happening.

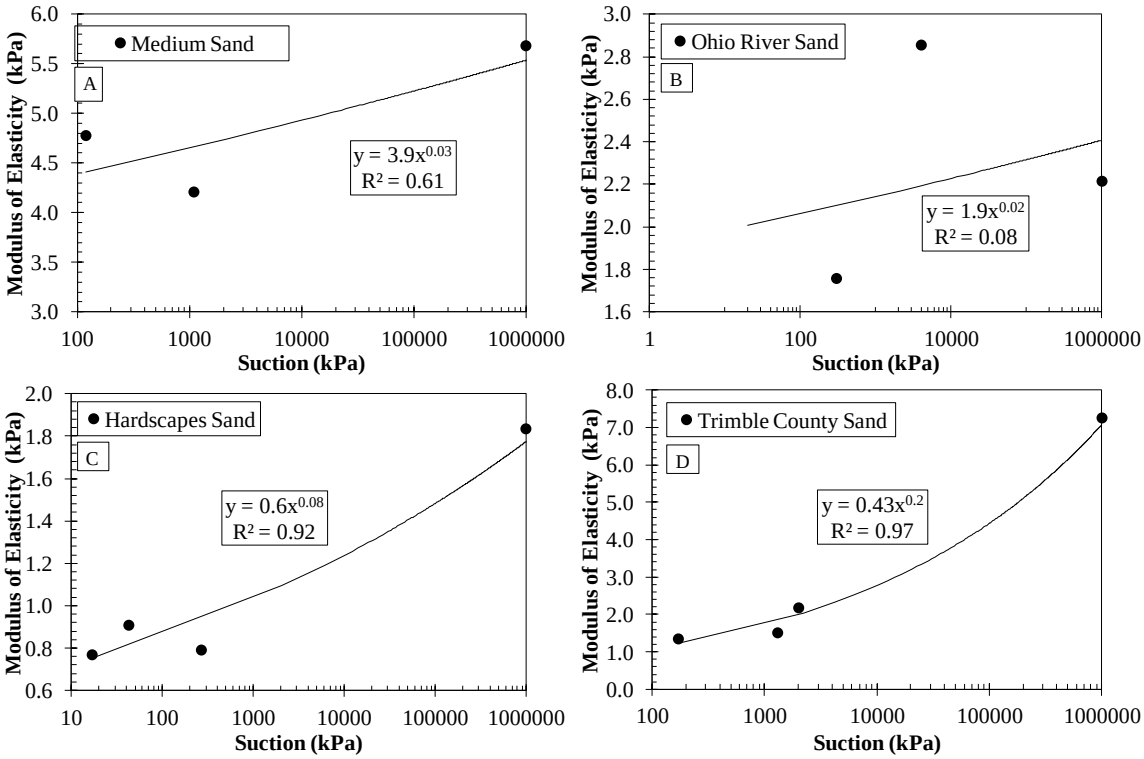

Figure 3.15. Compressive Strength versus Degree of Saturation.

In situ moisture, and in this case the suction due to moisture, affected grouted sand modulus of elasticity for several of reasons. Dry soil samples have a matric suction of 1,000,000 kPa. In these dry soils, the sand particles may have a tendency to adsorb grout moisture. This will result in a grout with decreased water in the pore space. As it applied to the modulus of elasticity, this will result in larger strength increases with strain. Furthermore, partially saturated soils will cause dilution of the grout. Indicative of lower modulus of elasticity values, increased dilution due to moisture will negatively affect the grout strength, (Perret et al., 2000). While initial moisture can play a crucial role in grout strength, an index that takes initial soil properties, density components, and moisture into effect may be useful in prediction of grouted sand strength. This is why suction is a beneficial indicator of strength in grout sands with variable initial moisture.

Matric suction has commonly been plotted versus the soil strength for analysis (Fredlund and Xing, 1994). However, Figure 3.16 shows that the initial soil suction in this experiment can be used to estimate strength of grouted sand specimens. Several samples were excluded in Figure 3.16. One sample, as previously described, was omitted because

the effluent filter broke. ASTM D4219 recommends injection pressures lower than 68.9 kilopascals for chemical grouted sands. The remaining samples were excluded from the relationship because to variable injection pressures, higher than desired, were necessary to grout the samples. This may have been due to the high compaction effort needed to compact the sample to the constant unit weight used in this study. The samples included in the relationship were obtained using without any malfunction or change in injection pressure, and were strictly in accordance to ASTM procedures.

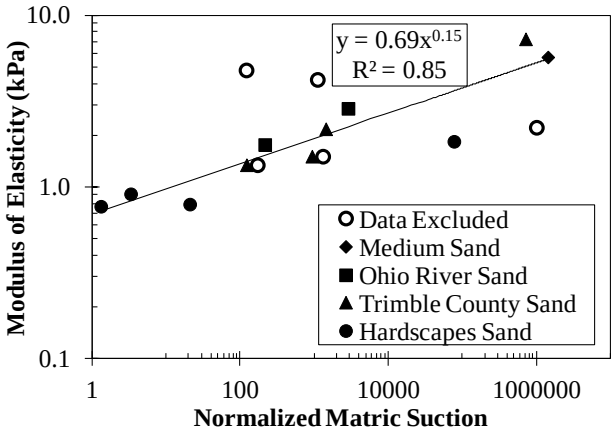

Figure 3.16. Modulus of Elasticity versus Normalized Matric Suction.

The relationship between normalized unconfined compressive strength and normalized suction is

$$E = a_1(\psi_n)^{a_2} \tag{34}$$

where E is the grouted sand elastic modulus, ψ_e is the effective soil suction, and a_1 and a_2 are empirical constants for the power function. In the power function constants, $a_1 = 0.69$ and $a_2 = 0.15$. Constant a_1 was an empirically estimated modulus at dry conditions. This represents dry conditions because the suction was normalized to the dry suction. Since a_2 was below one and negative, the power function increased at a decreasing rate of increase. There are several factors that governed this behavior. One was that the dry samples exert some adsorption on the grout mix and adsorbs some of the grout water. This causes the grout in dry conditions to have less moisture than in the initial mix. In the sand samples with partially saturated initial conditions, non-continuous water and air voids were in the pore space. This results in some mixing. This differs from to saturated

conditions where the pore space water gets replaced, nearly completely, by grout. This occurs because, under pressure, the water in the pores completely exits as the grout enters the pore space. A third reason was the capillary effects due to matric suction. It has been observed that as sands become less saturated they exhibit higher matric suction values, which results in higher strength. This initial condition of the grout likely applies to a resulting grouted sand, which this study provided evidence through this equation

Equation 32 contains an effective suction. This value was normalized in order to allow different units to be compared to this research, and so that the constant, a_1 pertains to pertinent dry conditions. Normalized suction is

$$\psi_n = \frac{\psi}{\psi_{aev}} \tag{35}$$

where ψ is the matric suction corresponding to the initial volumetric moisture content and ψ_{aev} is the matric suction air entry value. Both suction and air entry value was obtained from the SWCC, as previously described. Equation 32 is valid for the conditions in this study. Additional research will be necessary to continue developing these relations for all initial conditions possible in the field.

3.6 Conclusion

The influence of initial conditions on grouted sand properties, such as moisture content and variation in grain size, were evaluated. The grouted sand properties were investigated how these aspects influences grout penetration into the soil and the resulting grouted sand strength. Also, of grout mix ratios were investigated in respect to acrylate grout gel times. The conclusion drawn from this study are as follows:

- Unsaturated hydraulic conductivity increases with volumetric moisture and decreases with normalized suction.
- Normalized temperature decreased, by as much as 20 perent, as inhibitor concentrations are increased to only 0.15 percent of the total grout mix.
- The normalized temperature was largest at low ambient temperatures. This was indicative of a higher amount of increase from the ambient temperature. However, the maximum temperature was higher at higher ambient temperatures.

- At an inhibitor concentration of 0.15 percent, gel times increased from about 15 to 45 minutes as temperature increased from 15 to 25 degrees Celsius.
- Gel times decreased as inhibitor concentrations increased. With no inhibitor, the reaction only took seconds to take place. With only small amounts of inhibitor (ie. 0.15 percent) the gel time increased to as much as 45 minutes.
- Sands on the order of 10^{-4} cm/s are considered moderately groutable. One sand investigated in this study, with a hydraulic conductivity of 2.5×10^{-4} cm/s, was not groutable. This may be the case, circumstantially, for soils considered moderately groutable.
- Grout penetration increased by a factor of 2 as volumetric water content increased from dry conditions to a gravimetric moisture content of nine percent. This trend was expected, as soils with lower volumetric contents had lower hydraulic conductivities.
- Initial penetration rate relationships were developed for the soils used in this study. The factor used to form this relationship was comprised of grout properties, soil properties, and hydraulic conductivities. As an increased range of soil conditions are tested, this relationship may be expanded.
- Grouted sand modulus of elasticity decreased by as much as 80 percent as the fines content decreased from 4 to 1 percent.
- Increases in volumetric moisture content caused the grouted sand modulus of elasticity to decrease, in general. This was due to adsorption at near-dry conditions and dilution at partially saturated conditions.
- The elastic modulus of the grouted sands increased by about 7 kPa as normalized matric suction increased from 17 to 1,000,000 kPa. An empirical relationship was developed from the data investigated. This relationship was specific for the ranges of suction in this study, and has potential for expansion with additional data for additional in situ initial conditions.

CHAPTER 4

4 Conclusions

4.1 Mechanical Behavior of Ultrafine-Grouted Sands

The influence of initial conditions on grouted sand properties, such as moisture content and variation in grain size, were evaluated. The grouted sand properties were investigated how these aspects influences grout penetration into the soil and the resulting grouted sand strength. Also, influent of water-to-cement ratios were investigated in respect to neat grout specimens. The conclusions drawn from this study are as follows:

- Unsaturated hydraulic conductivity increases (ie. from 8.9×10^{-4} cm/s to 2.0×10^{-2}) with changes in graviemtric moisture from zero to nine percent. Matric suction was used to estimate the unsaturated moisture content.
- Increases in water-to-cement ratio have a significant effect on bleed. Increasing the water-to-cement ratio from one to four increased bleed from zero percent to 50 percent, causing the grout to be unstable. Similar changes in the water-to-cement ratio decreased the unconfined compressive strength by a factor of ten.
- As discussed, previous studies have shown that soils with five percent fines can be ungroutable. In this study, fine sand with eleven percent fines was investigated. This particular sand was not groutable. By all groutability criteria, this sand was considered moderately groutable. These results affirm assertions of previous studies that sand considered moderately groutable may not be groutable.
- Grout penetration rates through the sample increased, by as much as a factor of eight, as volumetric moisture increased from dry conditions to nine percent moisture. The observed grout penetration increase was directly related to unsaturated hydraulic conductivity. Relationships regarding injection and soil properties can be used in conjunction with hydraulic conductivity to develop relationships in initial penetration rates.
- Grouted sand strength decreased as moisture increased. A 50 percent decrease in strength was observed with an increase of nine percent gravimetric moisture. This was likely due to mixing of pore water and the grout suspension.

- With greater proportions of grout to initial soil and water, strength increases were seen. As the initial suction increased from about 50 to 1,000,000 kPa, the grouted sand strength increased by 150 percent. The soil-water characteristic curves are dependent upon the unit weight and soil-specific particle sizes. The specific soil suctions were selected from the appropriate initial moisture of the soil. This allows for grouted sand strength relationships based on soil matric suction.

4.2 Mechanical Behavior of Acrylate-Grout Sands

The influence of initial conditions on grouted sand properties, such as moisture content and variation in grain size, were evaluated. The grouted sand properties were investigated how these aspects influences grout penetration into the soil and the resulting grouted sand strength. Also, of grout mix ratios were investigated in respect to acrylate grout gel times. The conclusions drawn from this study are as follows:

- Unsaturated hydraulic conductivity increases with volumetric moisture and decreases with normalized suction.
- Normalized temperature decreased, by as much as 20 perent, as inhibitor concentrations are increased to only 0.15 percent of the total grout mix.
- The normalized temperature was largest at low ambient temperatures. This was indicative of a higher amount of increase from the ambient temperature. However, the maximum temperature was higher at higher ambient temperatures.
- At an inhibitor concentration of 0.15 percent, gel times increased from about 15 to 45 minutes as temperature increased from 15 to 25 degrees Celsius.
- Gel times decreased as inhibitor concentrations increased. With no inhibitor, the reaction only took seconds to take place. With only small amounts of inhibitor (ie. 0.15 percent) the gel time increased to as much as 45 minutes.
- Sands on the order of 10^{-4} cm/s are considered moderately groutable. One sand investigated in this study, with a hydraulic conductivity of 2.5×10^{-4} cm/s, was not groutable. This may be the case, circumstantially, for soils considered moderately groutable.
- Grout penetration increased by a factor of 2 as volumetric water content increased from dry conditions to a gravimetric moisture content of nine percent. This trend

was expected, as soils with lower volumetric contents had lower hydraulic conductivities.

- Initial penetration rate relationships were developed for the soils used in this study. The factor used to form this relationship was comprised of grout properties, soil properties, and hydraulic conductivities. As an increased range of soil conditions are tested, this relationship may be expanded.
- Grouted sand modulus of elasticity decreased by as much as 80 percent as the fines content decreased from 4 to 1 percent.
- Increases in volumetric moisture content caused the grouted sand modulus of elasticity to decrease, in general. This was due to adsorption at near-dry conditions and dilution at partially saturated conditions.
- The elastic modulus of the grouted sands increased by about 7 kPa as normalized matric suction increased from 17 to 1,000,000 kPa. An empirical relationship was developed from the data investigated. This relationship was specific for the ranges of suction in this study, and has potential for expansion with additional data for additional in situ initial conditions.

4.3 Future Research

Future work in this area should expand the limitations of initial conditions investigated and should be geared towards practical applications. Even if the general effects of initial conditions are understood, future research will be beneficial to grouting in that it can quantify grout flow distances and the resulting grouted sand permeability and strength. Studies involving grout mix design may also be beneficial to grouting procedures and implementation. Investigation into the effects of various additives on the grout effectiveness measures may be beneficial. Additives may be useful if the cost of the additive can be offset by benefits the additive may provide. While studies on the initial conditions will help with strength and considerations, they also may be helpful in predicting the effectiveness of field techniques and procedures.

Research concerning grouting techniques involving laboratory scale models will likely depict problems to be encountered in the field. This research may also provide quantification techniques to predict grout flow characteristics, permeability, and strength.

There should be investigations regarding correlations between grouted cylinder sample testing and application techniques. A laboratory study involving grouting cylinders, as performed in this study, and performing laboratory scale modeling of field applications may begin to provide relationships between testing procedures and laboratory implementation.

Appendix A

Soil Test Data

A.1 Grain Size Distribution

Table A.1. Grain Size Distribution for Kentucky River Sand.

Kentucky River Sand							
Sieve #	**Sieve size (mm)**	Weight-sieve+soil (grams)	Weight - Sieve (grams)	Weight - Soil (grams)	Percent Retained	Cumulative Percent Retained	Percent Finer
3/8"	9.50						
No. 4	4.75	517.1	517.1	0.0	0.00	0.00	100.0
No. 10	2.00	481.2	481.3	0.0	0.00	0.00	100.0
No. 20	0.85	428.5	428.2	0.3	0.06	0.06	99.9
No. 40	0.43	396.8	395.5	1.3	0.26	0.32	99.7
No. 60	0.25	592.9	537.9	55.0	10.98	11.30	88.7
No. 100	0.15	792.3	512.3	280.0	55.91	67.21	32.8
No. 140	0.11	539.3	463	76.3	15.24	82.45	17.6
No. 200	0.08	358.4	326.5	31.9	6.37	88.82	11.2
Pan	0.0			56.0	11.18	100.00	

Table A.2. Grain Size Distribution for Hardscapes Sand.

Hardscapes Sand							
Sieve #	**Sieve size (mm)**	Weight-sieve+soil (grams)	Weight - Sieve (grams)	Weight - Soil (grams)	Percent Retained	Cumulative Percent Retained	Percent Finer
3/8"	9.500						
No. 4	4.750	517.1	517.1	0.0	0.00	0.00	100.00
No. 10	2.000	482.1	481.3	0.8	0.16	0.16	99.84
No. 20	0.850	487.2	428.2	59.0	11.76	11.92	88.08
No. 40	0.425	586.3	395.5	190.8	38.03	49.95	50.05
No. 60	0.250	709.4	537.9	171.5	34.19	84.14	15.86
No. 100	0.150	576.7	512.3	64.4	12.84	96.98	3.02
No. 140	0.106	471	463	8.0	1.59	98.57	1.43
No. 200	0.075	328.4	326.5	1.9	0.38	98.95	1.05
Pan	0.000			5.3	1.05	100.00	

Table A.3. Grain Size Distribution for Ohio River Sand.

Ohio River Sand							
Sieve #	**Sieve size (mm)**	Weight-sieve+soil (grams)	Weight - Sieve (grams)	Weight - Soil (grams)	Percent Retained	Cumulative Percent Retained	Percent Finer
3/8"	9.500						
No. 4	4.750	522.3	517.1	5.2	1.04	1.04	100.00
No. 10	2.000	541.5	481	60.5	12.11	13.15	86.85
No. 20	0.850	534.1	428.2	105.9	21.19	34.34	65.66
No. 40	0.425	579.3	395.5	183.8	36.78	71.12	28.88
No. 60	0.250	635.2	537.1	98.1	19.63	90.75	9.25
No. 100	0.150	532.3	512.3	20.0	4.00	94.75	5.25
No. 140	0.106	465.9	462.6	3.3	0.66	95.41	4.59
No. 200	0.075	328.1	326.5	1.6	0.32	95.73	4.27
Pan	0.000			21.3	4.27	100.00	

Table A.4. Grain Size Distribution for Trimble County Sand.

Trimble County Sand							
Sieve #	**Sieve size (mm)**	Weight-sieve+soil (grams)	Weight - Sieve (grams)	Weight - Soil (grams)	Percent Retained	Cumulative Percent Retained	Percent Finer
3/8"	9.500						
No. 4	4.750	517.1	517.1	0.0	0.00	0.00	100.00
No. 10	2.000	500.3	480	20.3	4.04	4.04	95.96
No. 20	0.850	504.7	428.5	76.2	15.18	19.23	80.77
No. 40	0.425	558.9	395.8	163.1	32.50	51.72	48.28
No. 60	0.250	702.9	537	165.9	33.06	84.78	15.22
No. 100	0.150	564	512.3	51.7	10.30	95.08	4.92
No. 140	0.106	469.2	463.1	6.1	1.22	96.30	3.70
No. 200	0.075	330.2	326.7	3.5	0.70	96.99	3.01
Pan	0.000			15.1	3.01	100.00	

Table A.5. Grain Size Distribution for Medium Sand.

Medium Sand							
Sieve #	**Sieve size (mm)**	Weight-sieve+soil (grams)	Weight - Sieve (grams)	Weight - Soil (grams)	Percent Retained	Cumulative Percent Retained	Percent Finer
3/8"	9.50						
No. 4	4.75	517.1	517.1	0.0	0.00	0.00	100.0
No. 10	2.00	481	480	1.0	0.20	0.20	99.8
No. 20	0.85	447.91	428.13	19.8	3.96	4.16	95.8
No. 40	0.43	554.95	373.5	181.5	36.29	40.45	59.6
No. 60	0.25	745.51	538.6	206.9	41.38	81.83	18.2
No. 100	0.15	575.01	512.18	62.8	12.57	94.39	5.6
No. 140	0.11	468.8	462.31	6.5	1.30	95.69	4.3
No. 200	0.08	375.59	373.31	2.3	0.46	96.15	3.9
Pan	0.0			19.3	3.86	100.01	

A.2 Specific Gravity Data

Table A.6. Trimble County Sand Specific Gravity.

Soil Description	Trimble County Sand					
Pecometer Number	1		2		3	
Nominal Pycometer Volume	500	ml	500	ml	500	ml
Oven Dry Weight of Soil	100	g	100	g	100	g
Weight of Pycometer+ Water	663.57	g	659.61	g	661.2	g
Weight of Pycometer+ Water+Soil	725.99	g	722.02	g	723.75	g
Temperature	20	deg. Cels	20	deg. Cels	20	deg. Cels
Correction Factor K	1		1		1	
Specific Gravity	2.64		2.67		2.66	

Table A.7. Kentucky River Sand Specific Gravity.

Soil Description	Kentucky River Sand					
Pecometer Number	1		2		3	
Nominal Pycometer Volume	500	ml	500	ml	500	ml
Oven Dry Weight of Soil	99.5	g	96.3	g	88.7	g
Weight of Pycometer+ Water	665	g	660.7	g	662.6	g
Weight of Pycometer+ Water+Soil	727.4	g	721.1	g	718.4	g
Temperature	20	deg. Cels	20	deg. Cels	20	deg. Cels
Correction Factor K	1		1		1	
Specific Gravity	2.68		2.68		2.70	

Table A.8. Ohio River Sand Specific Gravity.

Soil Description	ORS					
Pecometer Number	1		2		3	
Nominal Pycometer Volume	500	ml	500	ml	500	ml
Oven Dry Weight of Soil	100	g	100	g	100	g
Weight of Pycometer+ Water	663.5	g	659.61	g	661.2	g
Weight of Pycometer+ Water+Soil	725.99	g	722.02	g	723.75	g
Temperature	20	deg. Cels	20	deg. Cels	20	deg. Cels
Correction Factor K	1		1		1	
Specific Gravity	2.66		2.66		2.66	

Table A.9. Ohio River Sand Specific Gravity.

Soil Description	Medium Sand					
Pecometer Number	1		2		2	
Nominal Pycometer Volume	500	ml	500	ml	500	ml
Oven Dry Weight of Soil	100	g	100	g	100	g
Weight of Pycometer+ Water	663.63	g	659.67	g	659.67	g
Weight of Pycometer+ Water+Soil	726.35	g	722.24	g	721.62	g
Temperature	20	deg. Cels	20	deg. Cels	20	deg. Cels
Correction Factor K	1		1		1	
Specific Gravity	2.68		2.67		2.63	

Table A.10. Hardscapes Sand Specific Gravity.

Soil Description	Hardscapes Sand					
Pecometer Number	1		2		3	
Nominal Pycometer Volume	500	ml	500	ml	500	ml
Oven Dry Weight of Soil	100	g	100	g	100	g
Weight of Pycometer+ Water	663.63	g	659.67	g	661.36	g
Weight of Pycometer+ Water+Soil	725.97	g	721.88	g	723.68	g
Temperature	20	deg. Cels	20	deg. Cels	20	deg. Cels
Correction Factor K	1		1		1	
Specific Gravity	2.66		2.65		2.65	

A.3 Hydraulic Conductivity Data

Table A.11. Hardscapes Sand Hydraulic Conductivity.

MEASUREMENTS AND CALCULATIONS				Hardscapes Sand		
Test No.	Head Loss (Δh)	Hydraulic Gradient (i)	Flow Volume (Q)	Time (t)	Flow Rate (q)	Hydraulic Conductivity (k)
#	cm	L/L	mL	s	cm^3/s	cm/s
1	83	6.54	500	47.98	10.42101	3.5E-02
2	83	6.54	500	47.36	10.55743	3.5E-02
3	83	6.54	500	47.5	10.52632	3.5E-02
4	83	6.54	500	47.6	10.5042	3.5E-02

Table A.12. Kentucky River Sand Hydraulic Conductivity.

MEASUREMENTS AND CALCULATIONS				Kentucky River Sand		
Test No.	Head Loss (Δh)	Hydraulic Gradient (i)	Flow Volume (Q)	Time (t)	Flow Rate (q)	Hydraulic Conductivity (k)
#	cm	L/L	mL	s	cm^3/s	cm/s
1	122	10.67	88	809	0.108776	2.2E-04
2	122	10.67	80	630	0.126984	2.6E-04
3	122	10.67	85	657	0.129376	2.7E-04
4	122	10.67	77	680	0.113235	2.3E-04
	122	10.67	60	533	0.11257	2.3E-04

Table A.13. Trimble County Sand Hydraulic Conductivity.

MEASUREMENTS AND CALCULATIONS				Trimble County Sand		
Test No.	Head Loss (Δh)	Hydraulic Gradient (i)	Flow Volume (Q)	Time (t)	Flow Rate (q)	Hydraulic Conductivity (k)
#	cm	L/L	mL	s	cm^3/s	cm/s
1	106	8.42	1000	68.88	14.518	3.8E-02
2	106	8.42	1000	68.8	14.53488	3.8E-02
3	106	8.42	1000	68.65	14.56664	3.8E-02
4	106	8.42	1000	68.5	14.59854	3.8E-02
5	106	8.42	1000	69.38	14.41338	3.7E-02

Table A.14. Ohio River Sand Hydraulic Conductivity.

MEASUREMENTS AND CALCULATIONS				Ohio River Sand		
Test No.	Head Loss (Δh)	Hydraulic Gradient (i)	Flow Volume (Q)	Time (t)	Flow Rate (q)	Hydraulic Conductivity (k)
#	cm	L/L	mL	s	cm^3/s	cm/s
1	106	8.42	1000	58.81	17.00391	4.4E-02
2	106	8.42	1000	59.93	16.68613	4.3E-02
3	106	8.42	1000	58.45	17.10864	4.4E-02
4	106	8.42	1000	59.05	16.9348	4.4E-02

Table A.15. Medium Sand Hydraulic Conductivity.

MEASUREMENTS AND CALCULATIONS				Medium Sand		
Test No.	Head Loss (Δh)	Hydraulic Gradient (i)	Flow Volume (Q)	Time (t)	Flow Rate (q)	Hydraulic Conductivity (k)
#	cm	L/L	mL	s	cm^3/s	cm/s
1	108.4	8.61	1000	101	9.90099	2.5E-02
2	108.4	8.61	1000	101	9.90099	2.5E-02
3	108.4	8.61	1000	102	9.803922	2.5E-02

Appendix B

Pure Grout Testing

B.1 Neat Ultrafine Cement Test Results

Table B.1. Neat Grout Bleed Test Results

Water-to Cement Ratio	Cement +Water Height (in)	Cement Height (in)	Percent Bleed (%)	Study
1	6	6	0	This Study
2	5.4375	5	8	This Study
3	6.4375	4.0625	37	This Study
4	6.75	3.5625	47	This Study
1	5.0625	5.0625	0	This Study
2	6.125	5.6875	7	This Study
3	6.4375	4.125	36	This Study
4	7.3125	3.75	49	This Study
3	11.76	7.27	38	Henn (2010)
4	11.76	5.75	51	Henn (2010)

Table B.2. Neat Grout Unconfined Compressive Strength Results.

Water-to-Cement Ratio	Compressive Strength (kPa)	Study
1	5709	This Study
1.5	1323	This Study
2	577	This Study
2.5	74	This Study
0.6	14200	Henn (2010)

B.2 Acrylate Gel Testing

Table B.3. Temperature-Time Data at 15 Degrees Celsius and 0 Percent KFe

0.0 % KFe			
Time (s)	t/t_{max}	Temp (deg Cels)	T/T_0
0	0.0	15	1.0
35	0.1	15	1.0
50	0.1	16	1.1
65	0.1	17	1.1
75	0.2	18	1.2
90	0.2	19	1.3
105	0.2	20	1.3
135	0.3	22	1.5
150	0.3	23	1.5
163	0.4	24	1.6
178	0.4	25	1.7
195	0.4	26	1.7
210	0.5	27	1.8
230	0.5	28	1.9
250	0.6	29	1.9
275	0.6	30	2.0
305	0.7	30.5	2.0
325	0.7	31	2.1
350	0.8	31.5	2.1
440	1.0	32	2.1
555	1.3	31.5	2.1
630	1.4	31	2.1

Table B.4. Temperature-Time Data at 15 Degrees Celsius and 0.05 Percent KFe

0.05 % KFe			
Time (s)	t/t_{max}	Temp (deg Cels)	T/T_0
0	0	15	1
540	0.514286	15	1
600	0.571429	16	1.066667
620	0.590476	17	1.133333
640	0.609524	18	1.2
680	0.647619	20	1.333333
700	0.666667	21	1.4
720	0.685714	22	1.466667
740	0.704762	23	1.533333
785	0.747619	24	1.6
810	0.771429	25	1.666667
840	0.8	26	1.733333
890	0.847619	27	1.8
920	0.87619	28	1.866667
960	0.914286	29	1.933333
1050	1	29.5	1.966667
1275	1.214286	29	1.933333
1395	1.328571	28.5	1.9

Table B.5. Temperature-Time Data at 15 Degrees Celsius and 0.10 Percent KFe

0.1 % KFe			
Time (s)	t/t_{max}	Temp (deg Cels)	T/T_0
0	0	15	1
1050	0.664557	16	1.066667
1090	0.689873	17	1.133333
1120	0.708861	18	1.2
1150	0.727848	19	1.266667
1180	0.746835	20	1.333333
1210	0.765823	21	1.4
1230	0.778481	22	1.466667
1260	0.797468	23	1.533333
1350	0.85443	26	1.733333
1400	0.886076	27	1.8
1435	0.908228	27.5	1.833333
1480	0.936709	28	1.866667
1580	1	28.5	1.9
1800	1.139241	28	1.866667
1940	1.227848	27.5	1.833333

Table B.6. Temperature-Time Data at 15 Degrees Celsius and 0.15 Percent KFe

0.15 % KFe			
Time (s)	t/t_{max}	Temp (deg Cels)	T/T_0
0	0	15	1
1970	0.691228	15	1
2190	0.768421	15	1
2245	0.787719	16	1.066667
2310	0.810526	17	1.133333
2350	0.824561	18	1.2
2420	0.849123	19	1.266667
2460	0.863158	20	1.333333
2565	0.9	22	1.466667
2625	0.921053	23	1.533333
2715	0.952632	24.5	1.633333
2745	0.963158	25	1.666667
2850	1	25.5	1.7
3240	1.136842	25	1.666667
3435	1.205263	24.5	1.633333

Table B.7. Temperature-Time Data at 20 Degrees Celsius and 0 Percent KFe

0.0 % KFe			
Time (s)	t/t_{max}	Temp (deg Cels)	T/T_0
0	0.0	19	1.0
15	0.0	19	1.0
20	0.1	19	1.0
40	0.1	21	1.1
50	0.2	22	1.2
55	0.2	23	1.2
70	0.2	24	1.3
80	0.2	25	1.3
90	0.3	26	1.4
105	0.3	27	1.4
115	0.3	28	1.5
125	0.4	29	1.5
140	0.4	30	1.6
150	0.5	31	1.6
160	0.5	32	1.7
180	0.5	33	1.7
200	0.6	34	1.8
240	0.7	35	1.8
280	0.8	35.5	1.9
330	1.0	36	1.9
420	1.3	36	1.9
480	1.5	35.5	1.9
600	1.8	35	1.8

Table B.8. Temperature-Time Data at 20 Degrees Celsius and 0.05 Percent KFe

0.05 % KFe			
Time (s)	t/t_{max}	Temp (deg Cels)	T/T_0
0	0.0	19	1.0
210	0.3	19.5	1.0
300	0.4	20	1.1
345	0.5	21	1.1
360	0.5	22	1.2
365	0.5	23	1.2
375	0.5	24	1.3
385	0.6	25	1.3
410	0.6	27	1.4
425	0.6	28	1.5
440	0.6	29	1.5
460	0.7	31	1.6
480	0.7	32	1.7
500	0.7	33	1.7
520	0.8	33.5	1.8
540	0.8	34	1.8
600	0.9	35	1.8
690	1.0	35.5	1.9
840	1.2	35	1.8
960	1.4	34	1.8

Table B.9. Temperature-Time Data at 20 Degrees Celsius and 0.1 Percent KFe

0.1 % KFe			
Time (s)	t/t_{max}	Temp (deg Cels)	T/T_0
0	0.0	19	1.0
480	0.4	19.5	1.0
570	0.5	20	1.1
800	0.7	21	1.1
820	0.7	22	1.2
830	0.7	23	1.2
845	0.7	24	1.3
860	0.7	25	1.3
870	0.8	26	1.4
905	0.8	28	1.5
925	0.8	29	1.5
940	0.8	30	1.6
960	0.8	31	1.6
985	0.9	32	1.7
1015	0.9	33	1.7
1065	0.9	34	1.8
1155	1.0	35	1.8
1470	1.3	34	1.8

Table B.10. Temperature-Time Data at 20 Degrees Celsius and 0.15 Percent KFe

0.15 % KFe			
Time (s)	t/t_{max}	Temp (deg Cels)	T/T_0
0	0.0	18	1.0
120	0.1	18	1.0
600	0.4	18	1.0
900	0.6	18.5	1.0
1120	0.7	19	1.1
1140	0.8	20	1.1
1175	0.8	21	1.2
1190	0.8	22	1.2
1210	0.8	23	1.3
1230	0.8	24	1.3
1245	0.8	25	1.4
1290	0.8	27	1.5
1315	0.9	28	1.6
1340	0.9	29	1.6
1370	0.9	30	1.7
1420	0.9	31	1.7
1520	1.0	32	1.8
1620	1.1	32	1.8
1740	1.1	32	1.8
1980	1.3	31	1.7

Table B.11. Temperature-Time Data at 25 Degrees Celsius and 0 Percent KFe

0.0 % KFe			
Time (s)	t/t_{max}	Temp (deg Cels)	T/T_0
0	0.0	25	1.0
25	0.1	26	1.0
30	0.1	27	1.1
40	0.2	28	1.1
50	0.2	29	1.2
58	0.3	30	1.2
110	0.5	36	1.4
150	0.7	39	1.6
185	0.8	40	1.6
230	1.0	41	1.6
405	1.8	40.5	1.6
450	2.0	40	1.6

Table B.12. Temperature-Time Data at 25 Degrees Celsius and 0.05 Percent KFe

0.05 % KFe			
Time (s)	t/t_{max}	Temp (deg Cels)	T/T_0
0	0.0	25	1.0
80	0.2	25	1.0
180	0.4	25.5	1.0
240	0.5	26	1.0
250	0.5	27	1.1
265	0.6	28	1.1
325	0.7	33	1.3
350	0.7	35	1.4
365	0.8	36	1.4
380	0.8	37	1.5
405	0.8	38	1.5
435	0.9	39	1.6
450	0.9	39.5	1.6
480	1.0	40	1.6
600	1.3	40	1.6
720	1.5	40	1.6
780	1.6	39.5	1.6
820	1.7	39	1.6

Table B.13. Temperature-Time Data at 25 Degrees Celsius and 0.1 Percent KFe

0.1 % KFe			
Time (s)	t/t_{max}	Temp (deg Cels)	T/T_0
0	0.0	25	1
10	0.0	25.5	1.02
30	0.0	26	1.04
405	0.5	26.5	1.06
555	0.6	27	1.08
585	0.7	28	1.12
600	0.7	29	1.16
615	0.7	30	1.2
630	0.7	31	1.24
690	0.8	34	1.36
700	0.8	35	1.4
735	0.8	36	1.44
755	0.9	37	1.48
775	0.9	37.5	1.5
795	0.9	38	1.52
825	0.9	38.5	1.54
885	1.0	39	1.56
960	1.1	38.5	1.54
1000	1.1	38	1.52

Table B.14. Temperature-Time Data at 25 Degrees Celsius and 0.15 Percent KFe

0.15 % KFe			
Time (s)	t/t_{max}	Temp (deg Cels)	T/T_0
0	0.000	24	1.0
20	0.015	24.5	1.0
120	0.091	25	1.0
900	0.682	26	1.1
920	0.697	27	1.1
950	0.720	28	1.2
975	0.739	29	1.2
995	0.754	30	1.3
1015	0.769	31	1.3
1070	0.811	33	1.4
1120	0.848	34	1.4
1155	0.875	35	1.5
1320	1.000	36	1.5
1440	1.091	35.5	1.5
1500	1.136	35	1.5

Table B.15. Gel and Maximum Temperature Data at 15 Degrees Celsius.

	15		Degrees Celsius			
Concentration (%)	Starting, Atmospheric Temperature, T_0 (± 1)	Time to Reach Max Temp, t_{max}	Max Temp, Deg Celc	Gel Time (min)	Gel Time (min)	T_{max}/T_0
0	15	440	32.0	150	2.5	2.1
0.05	15	1050	29.5	740	12.3	2.0
0.1	15	1580	28.5	1260	21.0	1.9
0.15	15	2850	27.0	2655	44.3	1.8

Table B.16. Gel and Maximum Temperature Data at 20 Degrees Celsius.

	19		Degrees Celsius			
Concentration (%)	Starting, Atmospheric Temperature, T_0 (± 1)	Time to Reach Max Temp, t_{max}	Max Temp, Deg Celc	Gel Time (sec)	Gel Time (min)	T_{max}/T_0
0	19	330	36.0	120	2.0	1.9
0.05	19	690	35.5	380	6.3	1.9
0.1	19	1155	35.0	870	14.5	1.8
0.15	18	1520	32.0	1230	20.5	1.7

Table B.17. Gel and Maximum Temperature Data at 25 Degrees Celsius.

	25		Degrees Celsius			
Concentration (%)	Starting, Atmospheric Temperature, T_0 (± 1)	Time to Reach Max Temp, t_{max}	Max Temp, Deg Celc	Gel Time (sec)	Gel Time (min)	T_{max}/T_0
0	25	230	41.0	80	1.3	1.6
0.05	25	480	40.0	315	5.3	1.6
0.1	25	885	39.0	660	11.0	1.6
0.15	24	1320	36.0	1005	16.8	1.4

Appendix C

Grout Procedure and Penetration Data

C.1 Apparatus and Procedures

The sample was transferred from apparatus to rubber sheets. To do this, first the top base of the grout holding cell was removed. During this removal, hand pressure was used to keep pressure adequate between the mold and o-ring on the base. Vacuum grease was applied to the top of the mold once the top was removed. A rubber sheet was put on top of the mold, which was supported by a piece of wood the mold was then flipped to a position where the wood and rubber sheet are on bottom. To avoid losing grout, pressure must be applied to the piece of wood and mold to keep contact between the mold and rubber sheet. Typically, one hand was used to apply pressure on wood while the other was pushing the mold into the rubber sheet. Once the mold was flipped, pressure was kept on the mold and a rubber sheet and weight were place on top. This allowed the sample to set.

Figure C.1. Grout Setting Conditions.

Capping Compound Application

Step 1: Plug in sulfur heating pot. The electrical outlet was located to the right of the pot.

Figure C.2. Plug in Pot.

Step 2: Turn the temperature gauge to appropriate temperature. This was located on the side of the sulfur melting pot.

Figure C.3. Set Pot Temperature.

Step 3: Wait about an hour for sulfur capping compound to melt.

Figure C.4. Allow Compound to Melt.

Step 4: Assemble the mold.

Step 5: Insert the capping compound into the mold. Using the guide to keep the sample level, place the sample into the compound. To transport the compound from the pot to the mold, a pan can be used to keep the floor free from dripping sulfur compound. The pan can then be cleaned by using hammering the end scraper or screw driver into the bottom of the sulfer compound that was stuck to the pan.

Figure C.5. Pan, Hammer, and Scraper.

The mold will begin to set within fifteen seconds, so this must be a very smooth process. Since it was very time-dependent, errors may be common. In case of inadequate capping, trim the sample and do it again. Hardened excess mix was to be inserted back into pot to be melted. The hammer and chisel can also be used to softly tap the compound to be removed from the mold.

Figure C.6. Image of Sample Molding.

Step 5: Capping the opposite end of a cylindrical specimen may not be as straightforward, depending on sample length. For my samples the length was not more than the length of the guide. This can be observed in the above picture. This means the guide cannot be used for the second end. Instead, a level was used to keep the other end of the sample parallel to the end that was capped first.

Figure C.7. Level Check.

C.2 Ultrafine Flow Data

Table C.1. Ultrafine Grout Flow Data and Associated Parameters.

Sand Name	Porosity, n	Volumetric Water Content, θ (%)	Saturated Hydraulic Conductivity, k_{sat} (cm/s)	Unsaturated Hydraulic Conductivity, k_w (cm/s)	Grout Permeability Factor	Penetration Rate (m/s)
Medium Sand				4.0E-04		
Medium Sand	0.40	4.8	2.5E-02	1.2E-03	0.39	0.06
Medium Sand	0.40	9.6	2.5E-02	2.7E-03	0.90	0.05
Medium Sand	0.40	14.4	2.5E-02	5.1E-03	1.69	0.10
Ohio River Sand	0.40	0.0	4.4E-02	8.9E-04	0.17	0.04
Ohio River Sand	0.40	4.8	4.4E-02	4.4E-03	0.82	0.08
Ohio River Sand	0.40	9.6	4.4E-02	1.1E-02	2.09	0.07
Ohio River Sand	0.40	14.4	4.4E-02	2.0E-02	3.74	0.11
Hardscapes Sand	0.40	0.0	3.5E-02	1.4E-03	0.32	0.02
Hardscapes Sand	0.40	4.8	3.5E-02	1.4E-02	3.36	0.09
Hardscapes Sand	0.40	9.6	3.5E-02	2.4E-02	5.68	0.09
Hardscapes Sand	0.40	14.4	3.5E-02	3.4E-02	8.03	0.17
Trimble County	0.40	0.0	3.8E-02	7.6E-04	0.17	0.04
Trimble County	0.40	5.1	3.8E-02	2.3E-03	0.49	0.04
Trimble County	0.40	9.6	3.8E-02	5.0E-03	1.09	0.05
Trimble County	0.40	14.4	3.8E-02	9.0E-03	1.96	0.06

C.3 Acrylate Flow Data.

Table C.2. Acrylate Flow Data and Associated Parameters.

Sand Name	Volumetric Water Content, θ (%)	Saturated Hydraulic Conductivity, k_{sat} (cm/s)	Unsaturated Hydraulic Conductivity, k_w (cm/s)	Pressure Head (cm)	Permeability Factor	Penetration Rate (m/s)
Medium Sand	0.0	2.4E-02	4.9E-06	1055.1	0.0	0.01
Medium Sand	4.8	2.4E-02	5.3E-05			
Medium Sand	9.6	2.4E-02	2.9E-04	1758.5	2.6	0.03
Medium Sand	14.4	2.4E-02	9.1E-04	1406.8	6.7	
Ohio River Sand	0.0	4.4E-02	1.4E-04	703.4	0.3	0.02
Ohio River Sand	4.8	4.4E-02	1.2E-03	703.4	2.5	0.01
Ohio River Sand	9.6	4.4E-02	3.3E-03	703.4	6.8	0.03
Ohio River Sand	14.4	4.4E-02	8.0E-03	703.4	16.5	0.04
Hardscapes Sand	0.0	3.5E-02	2.2E-05	703.4	0.1	0.03
Hardscapes Sand	4.8	3.5E-02	1.4E-03	703.4	3.5	0.02
Hardscapes Sand	9.6	3.5E-02	3.4E-03	703.4	8.7	0.03
Hardscapes Sand	14.4	3.5E-02	5.2E-03	703.4	13.5	0.07
Trimble County	0.0	3.8E-02	1.7E-06	703.4	0.0	0.02
Trimble County	4.8	3.8E-02	1.0E-04	703.4	0.2	0.01
Trimble County	9.6	3.8E-02	1.4E-04	703.4	0.3	
Trimble County	14.4	3.8E-02	4.6E-04	703.4	1.1	

Appendix D

Unconfined Compressive Strength Data

D.1 Ultrafine Grouted sand Unconfined Compressive Strength Data

Table D.1. Ultrafine Grouted sand Strength and Associated Data.

Sand Name	Specific Surface Area	Fines	Volumetric Moisture Content	Max Strength	Normalized Compressive Strength, q_{gs}/q_g
Name	mm^{-1}	$	θ	PSI	
Medium Sand	20.7	3.9	0.0	53.9	0.6
Ohio River Sand	15.1	4.3	0.0	115.5	1.4
Trimble County Sand	17.8	3.0	0.0	72.8	0.9
Hardscapes Sand	19.1	1.0	0.0	74.8	0.9
Trimble County Sand	17.8	3.0	4.8	49.0	0.6
Hardscapes Sand	19.1	1.0	4.8	38.6	0.5
Ohio River Sand	15.1	4.3	4.8	54.0	0.6
Medium Sand	20.7	3.9	4.8	50.1	0.6
Hardscapes Sand	19.1	1.0	9.6	41.4	0.5
Trimble County Sand	17.8	3.0	9.6	40.1	0.5
Ohio River Sand	15.1	4.3	9.6	31.9	0.4
Medium Sand	20.7	3.9	9.6	53.7	0.6
Medium Sand	20.7	3.9	14.4	37.0	0.4
Ohio River Sand	15.1	4.3	14.4	33.0	0.4
Hardscapes Sand	19.1	1.0	14.4	34.4	0.4
Trimble County Sand	17.8	3.0	14.4	52.4	0.6

Table D.2. Ultrafine Grouted sand Strength and Suction Data.

Sand	Moisture	Suction, ψ	Normalized Matric Suction	Compressive Strength	Normalized Compressive Strength
Name	%	kPa		PSI	
Medium Sand	0	1000000	1	53.9	0.6
Medium Sand	3	20000	0.02	50.1	0.6
Medium Sand	6	1100	0.0011	53.7	0.6
Medium Sand	9	120	0.00012	37.0	0.4
Trimble County Sand	0	1000000	1	72.8	0.9
Trimble County Sand	3	2000	0.002	52.3	0.6
Trimble County Sand	6	1300	0.0013	40.1	0.5
Trimble County Sand	9	170	0.00017	52.4	0.6
Ohio River Sand	0	1000000	1	115.5	1.4
Ohio River Sand	3	4000	0.004	54.0	0.6
Ohio River Sand	6	300	0.0003	31.9	0.4
Ohio River Sand	9	20	0.00002	33.0	0.4
Hardscapes Sand	0	1000000	1	75.4	0.9
Hardscapes Sand	3	270	0.00027	38.6	0.5
Hardscapes Sand	6	43	0.000043	41.4	0.5
Hardscapes Sand	9	17	0.000017	34.4	0.4

D.2 Acrylate Grouted sand Unconfined Compressive Strength Data

Table D.3. Acrylate Grouted sand Strength and Associated Data.

Sand	Specific Surface Area	Fines	Volumetric Moisture Content	Modulus of Elasticity
Name	mm^{-1}	$	%	kPa
Medium Sand	20.66	3.9	0.0	6
Hardscapes Sand	19.11	1.0	0.0	2
Trimble County Sand	17.82	3.0	0.0	7
Ohio River Sand	15.1	4.3	0.0	2
Medium Sand	20.66	3.9	4.8	
Ohio River Sand	15.1	4.3	4.8	3
Hardscapes Sand	19.11	1.0	4.8	1
Trimble County Sand	17.82	3.0	4.8	2
Medium Sand	20.66	3.9	9.6	4
Hardscapes Sand	19.11	1.0	9.6	1
Trimble County Sand	17.82	3.0	9.6	2
Ohio River Sand	15.1	4.3	9.6	2
Ohio River Sand	15.1	4.3	14.4	
Hardscapes Sand	19.11	1.0	14.4	1
Trimble County Sand	17.82	3.0	14.4	1
Medium Sand	20.66	3.9	14.4	5

Table D.4. Ultrafine Grouted sand Strength and Suction Data.

Sand	Moisture	Volumetric Water Content	Suction, ψ	Normalized Matric Suction	Modulus of Elasticity
Name	%	%	kPa		kPa
Medium Sand	0	0.0	1000000	1	5.7
Medium Sand	3	4.8	20000	0.02	
Medium Sand	6	9.6	1100	0.0011	4.2
Medium Sand	9	14.4	120	0.00012	4.8
Trimble County Sand	0	0.0	1000000	1	2.2
Trimble County Sand	3	4.8	4000	0.004	2.9
Trimble County Sand	6	9.6	300	0.0003	1.8
Trimble County Sand	9	14.4	20	0.00002	
Hardscapes Sand	0	0.0	1000000	1	1.8
Hardscapes Sand	3	4.8	270	0.00027	0.8
Hardscapes Sand	6	9.6	43	0.000043	0.9
Hardscapes Sand	9	14.4	17	0.000017	0.8
Trimble County Sand	0	0.0	1000000	1	7.2
Trimble County Sand	3	4.8	2000	0.002	2.2
Trimble County Sand	6	9.6	1300	0.0013	1.5
Trimble County Sand	9	14.4	170	0.00017	1.3

Appendix E

Additional Information

Table E.1. Swagelok Fitting Part Numbers.

Swagelok		
Product	Quantity	Part No.
HEX NIPPLE	6	B-8-HN-8RT
On/off (two-way) Valves	4	40 series - 45F8
Elbow F-F	1	B-8-E
Elbow F-M	4	B-8-SE
Plugs	6	B-600-P
PFA Tubing	50`	PFA-T6-062-50

Table E.2. Products Ordered for This Study.

Website	Material	Part #	Price (each)	Quantity
Swagelok.com	On/off (two-way) Valves	BR2FT-050	$7.80	5
Swagelok.com	Elbow F-M	B-8-SE	$18.40	4
Swagelok.com	Tee	B-810-3-8TTM	$17.80	3
usplastic.com	Acrylic Tube	44036	17.22/6 ft	Least Cost
lowes.com	3/8" Threaded Rod	45479	$5.97	10'

Table E.3. Acrylic Mold Options.

Website	Material	Part #	Price	Information
mcmaster.com	Acrylic Tube	8486K345	22.52/ft	Most Cost
usplastic.com	Acrylic Tube	44036	17.22/6 ft	Least Cost
eplastics.com	Acrylic Tube	ACREXT2.250X2.000	37.47 for 6'	Will cut for us

Table E.4. Lexington O-Ring Distributor. Donated O-Rings.

Parker O-Ring Distributor		
Name	Email	Number
Billie	bharris@ibmoore.com	859-317-7235
Tim	thodges@ibmoore.com	859-317-7237

References

Abraham, A. (2006). "Effect of Initial Moisture State on the Engineering Properties of Microfine Cement Grouted Sands." *Master's thesis*, presented to University of Alabama at Huntsville, AL in partial fulfillment of the requirements of Master of Science

American Cyanamid. (1960). "Constructing Grout Curtain for Dam." *Technical Brief* Avanti International, Webster, TX.

Anagnostopoulos, C., and Hadjispyrou, S. (2004). "Laboratory Study of an Epoxy Resin Grouted Sand." *Ground Improvement*, 8(1), 39-45.

Avanti International. (2014A). "AV-160 SuperGel Technical Data Sheet." *AVANI International*, Webster, TX.

Avanti International. (2014B). "Potassium Ferricyanide Technical Data Sheet." *AVANI International*, Webster, TX.

Avanti Staff. (2014C). "Ultrafine Standard Technical Data Sheet." *AVANI International*, Webster, TX.

Axelsson, M. and Gustafson, G. (2007). "Grouting With High Water-Cement Ratios." *Report No. 2007:5*, Department of Civil and Environmental Engineering, Chalmers University of Technology, Gothenburg, Sweden.

Babcock, B. (2013A). "Cement Grout vs. Chemical Grout." *Geotechnical Division World Tunneling*, June 2013, 20-21.

Babcock, B. (2013B). "Sorting Out the Grout." *Geotechnical Division World Tunneling*, June 2013, 20-21.

Bell, F. (1993). *Engineering Treatment of Soils*. E and F N Spon. Boundary Row, London, UK.

Bolisetti, T., Reitsma, S., and Balachanar, R. (2009). "Experimental Investigations of Colloidal Silica Grouting in Porous Media." *Journal of Geotechnical and Geoenvironmental Engineering*, ASCE, 135 (5) 697-700

Bruce, D. (1992). "Progress and Developments in Dam Rehabilitation by Grouting." *Proc,. ASCE Special Proceedings: Grouting, Soil Improvement, and Geosynthetics.* New Orleans, LA, February 25-28 601-613

Campbell, G. (1974). "A Simple Method for Determining Unsaturated Conductivity from Moisture Retention Data." *Soil Science*, 117 (6), 311-314.

Christopher, B. R., Atmatzidis, D. K., and Krizek, R. J. (1989). "Laboratory testing of chemically grouted sand." *Geotechnical Testing Journal*, ASCE, 12(2), 109-118.

Clough, G. W., Kasali, G., and Kuck, W. (1979). "Silicate-stabilized sands." *Journal of the Soil Mechanics and Foundations Division*, 105(1), 65-82.

Dano, C., Hicher, P., and Tailliez, S. (2004). "Engineering Properties of Grouted Sands." *Journal of Geotechnical and Geoenvironmental Engineering*, ASCE, 130 (3) 38-338.

Delfosse-Ribay, E., Djeran-Maigre, I., Cabrillac, R., and Gouvenot, D. (2006). "Factors Affecting the Creep Behavior of Grouted Sands." *Journal of Geotechnical and Geoenvironmental Engineering*, ASCE, 132(4) 488-500.

ECO. (2014). "Mount Isa Mines: Stopping Water Inflow Into Pilot Holes for Raised Bore Using Acrylate." ECO Grouting Specialists, Inc. Amaranth, Ontario, Canada.

Fredlund, D.G. and Xing, A. (1994). "Equations for the Soil-Water Characteristic Curve." *Canadian Geotechnical Journal*, 31(4), 521-532.

Fredlund, M. (1999). "The Role of Unsaturated Soil Property Functions in the Practice of Unsaturated Soil Mechanics." *Doctoral Dissertation*, University of Saskatchewan, Saskatoon, Canada.

Fredlund, D. (2006). "Unsaturated Soil Mechanics in Engineering Practice." *Journal of Geotechnical and Geoenvironmental Engineering*, ASCE, 132 (3) 286-321

Fredlund, D., Rahardjo, H., and Fredlund, M. (2012). *Unsaturated Soil Mechanics in Engineering Practice.* John Wiley & Sons, Inc. Hoboken, NJ.

Gallagher, P. (2000). "Passive Site Remediation for Mitigation of Liquefaction Risk." *Doctoral Dissertation*, Virginia Polytechnic Institute and State University, Blacksburg, VA.

Gazaway, H., Coad, R., and Andromalos, K. (1991). “Installation of a Grout Curtain at a Hazardous Waste Landfill.” *Proc., Engineering Congress 1991*, ASCE, June 10 to 12, Boulder, CO.

Gentry, J. and Magill, D. (2012). “Acrylamide Grouting: Successfully Controlling Groundwater from Canada to South America.” *Proc., Fourth International Conference of Grouting and Deep Mixing*, ASCE, February 15-18, 1562-1568

Geo-Grout. (2008). “Permeation Grouting.” San Francisco, CA < http://www.geogroutinc.com/permeation_grouting.php>

Han, T. (2004). “Gel Time of Calcium Acrylate Grouting Material.” *Journal of Zhejiang University Science.* 5 (8) 928-931.

Hazen, A. (1892) ‘‘Some physical properties of sands and gravels, with special reference to their use in filtration.’’ *24th Annual Rep., Massachusetts State Board of Health*, Pub. Doc. No. 34, 539–556.

Henn, R. (2010) *Ultrafine Cement in Pressure Grouting.* American Society of Civil Engineers, Reston, VA .

Johnson, S. J. (1958). "Cement and Clay Grouting of Foundations: Grouting with Clay Cement.” *Journal of the Soil Mechanics and Foundation Engineering Division*, ASCE, (1545), 1-12.

Jury, W. and Horton, R. (2004). *Soil Physics: Sixth Addition.* John Wiley & Sons, Inc. Hobokan, NJ.

Karol, R. (2003). *Chemical Grouting and Soil Stabilization: Third Edition, Revised and Expanded*. Marcel Dekker, Inc. Basel, Switzerland.

Kim, Y. and Whittle, A. (2009). “Particle Network Model for Simulating the Filtration of a Microfine Cement Grout in Sand.” *Journal of Geotechnical and Geoenvironmental Engineering*, ASCE, 135 (2), 224-236.

Krizek, R., Michel, D., Helal, M., and Borden, R. (1992). “Engineering Properties of Acrylate Polymer Grout.” *Geotechnical Special Publication*, (30) 712-724.

Littlejohn, G. (1985). “Chemical Grouting.” *Ground Engineering,* 18 (2) 13-16; 18 (3) 23-28; 18 (4) 29-34.

Markou, N. and Droudakis, A. (2013). “Factors Affecting Engineering Properties of Microfine Cement Grouted Sands.” *Geotechnical and Geological Engineering*, 31 (4), 1041-1058.

Mitchell, J. K. (1970). "In-place Treatment of Foundation Soils." *Journal of the Soil Mechanics and Foundation Engineering Division,* ASCE, 96(1), 73-110.

Mollamahmutoglu, M. and Yilmaz, Y. (2011). “Engineering Properties of Medium-to-Fine Sands Injected with Microfine Cement Grout.” *Marine Georesources and Geotechnology*, (29) 95-109.

NAVFAC. (1983). “Dewatering and Ground Control.” *P-148* Navy Facilities Engineering Command, Washington, D. C.

Nonveiller, E. (1989). *Grouting Theory and Practice.* Elsevier Science Publishing Company, Inc. New York, NY

Ozgurel, H. and Vipulanandan, C. (2005). “Effect of Grain Size and Distribution on Permeability and Mechanical Behavior of Acrylamide Grouted Sand.” *Journal of Geotechnical and Geoenvironmental Engineering*, ASCE, 131 (12), 1457-1465.

Perret, S., Khayat, K., and Ballivy, G. (2000). “The Effect of Degree of Saturation of Sand on Groutability-Experimental Simulation.” *Ground Improvement*, (4), 13-22.

Persoff, P., Apps, J., Moridis, G., and Whang, J. (1999). “Effect of Dilution and Contaminants on Sand Grouted with Colloidal Silica.” *Journal of Geotechnical and Geoenvironmental Engineering*, ASCE, 125 (6), 461-469

Powers, J, Corwin, A., Schmall, P., and Kaeck, W. (2007). *Construction Dewatering and Groundwater Control, New Methods and Applications, Third edition.* Wiley, New York, NY.

Saada, C., Canou, J., Dormieux, L., and Dupla, J. (2006). “Evaluation of Elementary Filtration Properties of Cement Grout Injected in a Sand.” *Canadian Geotechnical Journal*, NRC Canada, 43 (1), 1273-1289.

Schiffman, R.L. and Wilson, C.R., (1958). "The Mechanical Behavior of Chemically Treated Grouted Soils." *Conference for grout and drilling method in engineering practice*, Butterwoths, London, UK, 29-35.

Schwarz, L. and Chirumalla, M. (2007). "Effect of Injection Pressure on Permability and Strength of Microfine Cement Grouted Sand." *Grouting for Ground Improvement* GeoDenver: 2007: New Peaks in Geotechnics. Denver, CO, February 18-21, 1-15

Scott, R. A. (1963). *Grouts and drilling muds in engineering practice*. Butterworths, London, England.

Soule, N. and Henn, R. (2010). *Ultrafine Cement in Pressure Grouting.* American Society of Civil Engineers Press, Reston, VA.

U.S Grout. (1999). "Ultrafine Cement Grout Seals Fissures in Salt Caverns." *Case History*, U.S.Grout, Webster, TX.

Uchikawa, H. (1994). "Ultra-Fine Cements for Special Applications." *Advanced Cement Based Materials*, 1(3) 150-154.

Vipulanandan, C. and Krizek, J. (1986). "Mechanical Behavior of Chemically Grouted Sands." *Journal of Geotechnical Engineering*, ASCE, 112 (9) 869-887

Vipulanandan, C., Ata, A., and Mebarkia, S. (1994). "Fracture Behavior of Cement Grouted Sand." *Proc., Specialty Conference on Grouting, Soil Improvement and Geosynthetics*, ASCE, (43) 147-159.

Warner, J. (2004). *Practical Handbook of Grouting: Soil, Rock, and Structures.* John Wiley & Sons, Inc. Hobokan, NJ.

Xanthakos, P., Abramson, L., and Bruce, D. (1994). *Ground Control and Improvement*. John Wiley & Sons, Inc. New York, NY

Zapata, C., Houston, W., Houston, S., and Walsh, K. (1999). "Soil-Water Characteristics Curve Variability." *Doctoral Disseration*, Arizona State University, Tempe, Arizona

Zapata, C.E., Houston, W.N., Houston, S.L., & Walsh, K.D. (1999). "Soil–Water Characteristic Curve Variability", Department of Civil and Environmental Engineering, Arizona State University.

Zebovitz, S., Krizek, R., and Atmatzidis, D. (1989). “Injection of Fine Sands with Very Fine Cement Grout.” *Journal of Geotechnical Engineering,* ASCE, 115(12), 1717-1733.

Vita

Ryan Ortiz was born and raised in Elizabethtown, Kentucky. He graduated from Central Hardin High School in 2009. Ryan attended the University of Kentucky and graduated with a Bachelor's of Science in Civil Engineering in 2013. He obtained his Engineering in Training (EIT) Certificate in May of 2013 in the State of Kentucky. He received Dean's List honors several semesters. Ryan was the recipient of the Presidential Scholarship and the William T. Parker Scholarship. During Graduate School at UK, he also received the Lyman T. Johnson Scholarship. Ryan is a co-author on two publications:

Bryson, L. and Ortiz, R. (2014). "Lab-Scale Study of Ultrafine Cement Grout Curtains Using a Physical Model." *Proc., Of Geo-Congress 2014,* ASCE, Va., 3252-3261.

Bryson, L., Ortiz, R., and Leandre, J. (2014). "Effects of a Grout Curtain on Hydraulic and Electrical Conductivity in a Laboratory-Scale Seepage Model." *Proc., Of Geo-Congress 2014*, ASCE, Va., 3233-3242.